THESIS FOR THE DEGREE OF LICENTIATE OF ENGINEERING

Conjugated polymers with functional side chains for photovoltaics

KIM BINI

Department of Chemistry and Chemical Engineering

CHALMERS UNIVERSITY OF TECHNOLOGY

Gothenburg, Sweden 2017

Conjugated polymers with functional side chains for photovoltaics

Kim Bini

Thesis for the Degree of Licentiate of Engineering

Chalmers University of Technology

Nr 2017:25

Department of Chemistry and Chemical Engineering

Division of Applied Chemistry

Chalmers University of Technology

412 96, Göteborg

Sverige

Telephone +46 (0) 31-772 1000

Cover:

TEM micrograph of polymer:PCBM blend after annealing. Produced with a FEI Tecnai T20 (LaB6, 200 kV) and processed with Gatan DigitalMicrograph V 3.21.

Chalmers Reproservice

Göteborg, Sverige, 2017

Conjugated polymers with functional side chains for photovoltaics

Kim Bini
Chalmers University of Technology
Department of Chemistry and Chemical Engineering

Abstract

Polymer solar cells are quickly approaching viability as a large scale electrical power source. To increase their stability and processability in green solvents, we want to modify their solubilizing side chains with different functionalities. Therefore, in this thesis, a several series of conjugated polymers are presented along with their characterization and utilization. A specific focus is put on the morphology characterization of polymer:PCBM-blends with the use of transmission electron microscopy, which can be a powerful tool to illuminate the bulk of materials where the morphology is of utmost importance. Three case studies are presented where polymer solar cells were characterized with this instrument along with the different conclusions that can be drawn from the data. Afterwards a series of conjugated random copolymers bearing thermocleavable side chains is presented with the purpose of introducing solvent processability which can be removed, leaving insoluble polymer films. They are characterized extensively and their thermal degradation is studied in detail. A morphological study is performed in order to analyze the effect the thermal stabilization has on the morphology and the pure thermocleavable polymer completely stabilized the film. In the following section, a series of fluorene based polymers with polar pendant groups were presented. The polymers were used as cathode interfacial material in all-polymer solar cells and increased the performance from 2.7% to a maximum of 5.4%, a level comparable to that of the inorganic lithium fluoride material. This method thus shows a good alternative for future high throughput production of solar cells. In a related project, similar polymers with varied energy levels were produced with the aim of studying their performance as active layer materials. Polymers bearing tertiary amines are common in interlayers, but not in active layers, due to hole trappingWhen tried in solar cells, one polymer showed a performance of above 1%. These results are a step towards polymer solar cell active layers processable in alcohol/water.

Keywords: conjugated polymers, polymer solar cells, side chain engineering, transmission electron microscopy, green solvent solubility

Acknowledgements

I would like to acknowledge the Swedish Research Council (VR) for funding my project.

I am grateful for the opportunity as well as the supervision from Dr. Ergang Wang and Prof. Mats Andersson. They have given me the chance to work in an exciting field, with great colleagues and friends.

On the same note, I greatly appreciate my colleagues at Chalmers, Dr. Xiaofeng Xu, Petri Murto, Zhaojun Li, Mariza Mone, Cedrik Wiberg, Wenjing Xiong and everyone else from the Diamond Division™ for giving me a great work environment with much fun and science. A special thank you is also required to Renee Kroon, my office mate, who allowed me to turn the office into a greenhouse without any complaints.

I would also like to take the opportunity to thank my collaborators Anirudh Sharma, Qingzhen Bian, Chuanfei Wang. A special thanks to Olof Bäcke, who spent many hours with me, teaching me how to use the TEM-instrument.

To my beloved wife Maria and my family: I could never do this without you. Thank you for all your support!

List of Publications

This thesis is based on the following publications:

Paper 1. Pyrrolo 3,4-g quinoxaline-6,8-dione-based conjugated copolymers for bulk heterojunction solar cells with high photovoltages
Xiaofeng Xu; C. F. Wang; O. Backe; David James; Kim Bini; E. Olsson; Mats R. Andersson; M. Fahlman; Ergang Wang
Polymer Chemistry, Vol. 6 (2015), 25, p. 4624-4633.

Paper 2. Effects of side chain isomerism on the physical and photovoltaic properties of indacenodithieno[3,2-b]thiophene–quinoxaline copolymers: toward a side chain design for enhanced photovoltaic performance
Xiaofeng Xu; Zhaojun Li; Olof Bäcke; Kim Bini; David James; Eva Olsson; Mats R. Andersson; Ergang Wang
Journal of Materials Chemistry, Vol. 2 (2014), 44, p. 18988-18997.

Paper 3. Low Band Gap Polymer Solar Cells With Minimal Voltage Losses
C. Wang; Xiaofeng Xu; W. Zhang; J. Bergqvist; Y. Xia; X. Meng; Kim Bini; W. Ma; A. Yartsev; K. Vandewal; Mats R. Andersson; O. Inganäs; M. Fahlman; Ergang Wang
Advanced Energy Materials, Vol. 6 (2016), p. 1600148.

Paper 4. Synthesis and of Isoindigo-based Polymers with Thermocleavable Side Chains
Kim Bini, Anirudh Sharma, Xiaofeng Xu, & Ergang Wang*
Manuscript, submitted.

Paper 5. Alcohol-Soluble Conjugated Polymers as Cathode Interlayers for All-Polymer Solar Cells
Kim Bini, Xiaofeng Xu, Mats. R. Andersson & Ergang Wang*
Manuscript

Paper 6. Conjugated Polymers with Tertiary Amine Pendant Groups for Organic Electronic Applications
Kim Bini, Xiaofeng Xu, Mats. R. Andersson & Ergang Wang*
Manuscript

Publications not included in this thesis:

Synthesis and characterization of benzodithiophene and benzotriazole-based polymers for photovoltaic applications
Desta Antenehe Gedefaw; M. Tessarolo; M. Bolognesi; M. Prosa; Renee Kroon; Wenliu Zhuang; Patrik Henriksson; Kim Bini; Ergang Wang; M. Muccini; M. Seri; Mats R. Andersson
Beilstein Journal of Organic Chemistry, Vol. 12 (2016), p. 1629-1637.

Contribution Report

Paper 1. Responsible for parts of the material characterization and TEM analysis.
Paper 2. Responsible for parts of the material characterization and TEM analysis.
Paper 3. Responsible for parts of the material characterization and TEM analysis.
Paper 4. Responsible for synthesis and most characterization. Responsible for writing the manuscript as first author.
Paper 5. Responsible for synthesis and characterization of interlayer polymers and manuscript writing manuscript as first author.
Paper 6. Responsible for synthesis and polymer characterization. Responsible for writing the manuscript as first author.

List of Acronyms

AFM – Atomic Force Microscopy
All-PSC – All-polymer solar cell
BTz – Benzotriazole
BHJ – Bulk heterojunction
t-BOC - tert-butyloxycarbonyl
CV – Cyclic Voltammetry
D-A – Donor Acceptor
DFT – Density functional theory
DIO – Diiodooctance
DMAP - Dimethylamino pyridine
DMF – Dimethylformamide
DPP – Diketopyrrolopyrrole
FF – Fill-factor
GPC – Gel permeation chromatography
HOMO - Highest occupied molecular orbital
II – Isoindigo
J_{SC} – Short-circuit current
LiF – Lithium Fluoride
LUMO – Lowest unoccupied molecular orbital
Mn – Number-averageverage molecular weight
Mw – Weight-average molecular weight
P3HT – Poly-3-hexyl thiophene
PEDOT:PSS – poly(3,4-ethylenedioxythiophene):polystyrene sulfonate
PCBM – Phenyl-C61-butyric acid methyl ester
PCE – Power conversion efficiency
PDI – Polydispersity index
$Pd_2(dba)_3$ – tris(dibenzylideneacetone)dipalladium(0)
$P(o\text{-}Tol)_3$ – tri(o-tolyl)phosphine
PSC – Polymer solar cell
SWV – Square wave voltammetry
TEM – Transmission electron microscopy
TGA – Thermogravimetric analysis
V_{OC} – Open-circuit voltage

Table of contents

Page intentionally left blank.

1. Introduction

We face large problems. The amount of CO_2-emissions remaining to stay below the 2-degree limit is rapidly decreasing. According to the International Energy Agency's World Energy Outlook Special Report from 2015, at the current rate that limit will be passed by 2040.[1] A graph of the progress is shown in figure 1.1. The need for new and sustainable is dire, but the outlook is not completely bleak. In the same report, it is mentioned that the increase in emissions is slowing down and investments in renewable energy are rapidly growing. Still, there is great need for further development of new technology to accelerate green energy production. One of the most promising energy sources is solar energy. The investments in solar energy production are steadily increasing,[1] but even with a rapidly decreasing solar cell prices, the initial investment is still daunting. It takes several years of operation before the energy and money is paid back for conventional solar panels.[2-3]

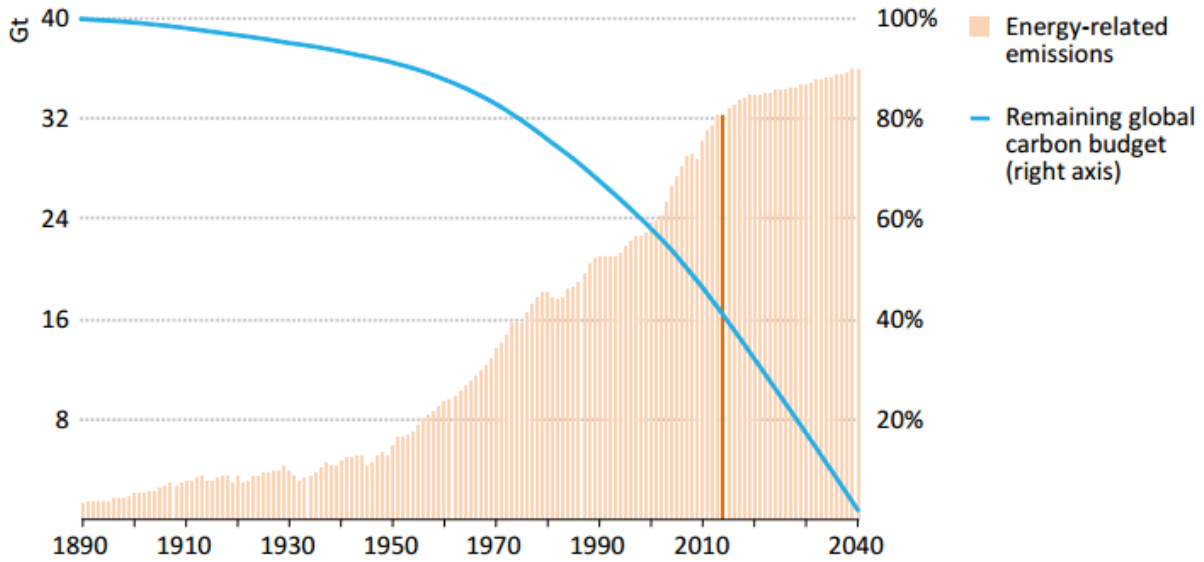

Figure 1.1. Global CO_2 emissions related to the remaining carbon budget for a >50% chance of clearing the 2 degree goal.[1]

Organic semiconductors grew to prominence by the end of last century with the promise of highly tunable, cheap and solution processable electronics. The properties of conjugated polymers enable a wide variety of interesting applications, such as light emitting diodes,[4] thermoelectric devices,[5] field-effect transistors[6] as well as for photovoltaics.[7] Making use of the solubility of polymers, large scale production is potentially far cheaper than production of conventional electronics.[7-10] The hope is to utilize these semiconducting polymers in photovoltaic devices as scalable green technology.

This thesis contains summary from three manuscripts, focused on side-chain engineering of conjugated polymers for organic photovoltaics. It begins, however, with a section that summarizes and compares parts of three publications, focusing on the morphological study of active layers using transmission electron microscopy.

In chapter 4 of this thesis, a method for introducing solvent resistance in a conjugated polymer film is presented. Making use of a common protecting functional group which is sensitive to heat, heat annealing the film makes it insoluble in any common solvent. This method has been applied to a common building block of conjugated polymers, namely the isoindigo (II) structure. This has been polymerized and characterized, studying the solubility, electrochemical and optical properties along with some produced conjugated polymers along with characterization of them.

After this study, a series of alcohol-soluble conjugated polymers aimed at interlayers for all-polymer solar cells (all-PSCs) is presented. In it, three polyfluorene- and one poly(fluorene-alt-phenylene) polymers are presented with three different amine containing pendant groups on their alkyl side chains. These polymers are used as cathode interlayers in all-PSCs with an active layer consisting of previously presented polymers with high performance. The interlayers are compared to conventional lithium fluoride(LiF)/Al electrode and found to perform just as well.

Finally, in chapter 6 a different use for tertiary amine pendant groups is studied. In this study, several conventional active layer donor-acceptor polymers were outfitted with tertiary amine pendant groups on their side chains. Amine containing polymers have been shown to be highly damaging for device performance, due to space charge buildup. This potentially enables a switchable solubility in the form of protonation/deprotonation. Theoretically this should enable processing with a weakly acidic alcohol solution with a volatile acid, which will evaporate and leave the polymer resistant to the next device layer solvent. Seven polymers based on benzotriazole (BTz), diketopyrrolopyrrole (DPP) and II are presented and one benzotriazole-based polymer showed a stable PCE of ~1%.

2. Organic photovoltaics

2.1 Solar Energy

The sun inundates the earth with vast amounts of electromagnetic radiation every day. The energy reaching the surface mostly consists of photons in the visible and infrared-region of the spectra, with wavelengths between 300 and 2000 nm with a long tail of light with ever longer wavelengths.[11] This light is essential to life on earth and is used by plants in photosynthesis to store chemical energy. It can also be utilized to generate electrical energy and heat. Due to the sheer amount of energy, a relatively small piece of the surface area of our planet could fulfill the entire global energy demand for the foreseeable future.

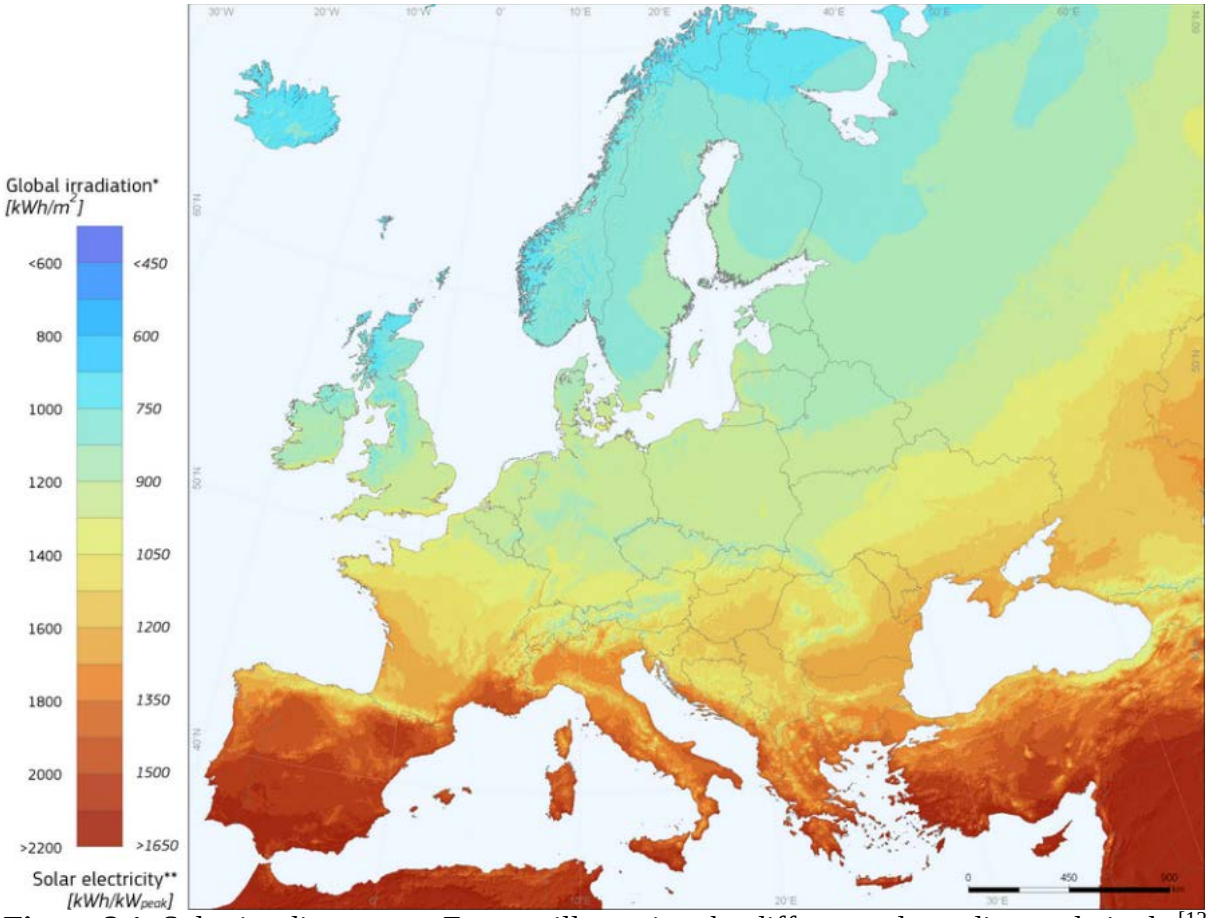

Figure 2.1. Solar irradiance over Europe, illustrating the difference depending on latitude.[12-13]

The solar energy is highly dependent on where on the globe you are, for example the closer to the equator the stronger inundation. As can be seen in figure 2.1 the dose of solar energy over Europe varies close to a factor of three from the north of Norway to the south of Spain. Nevertheless, for comparison there is a standard spectra of solar irradiation called the AM1.5G

solar radiation spectrum. This standard spectra, seen in figure 2.2, shows the importance of a wide absorption.

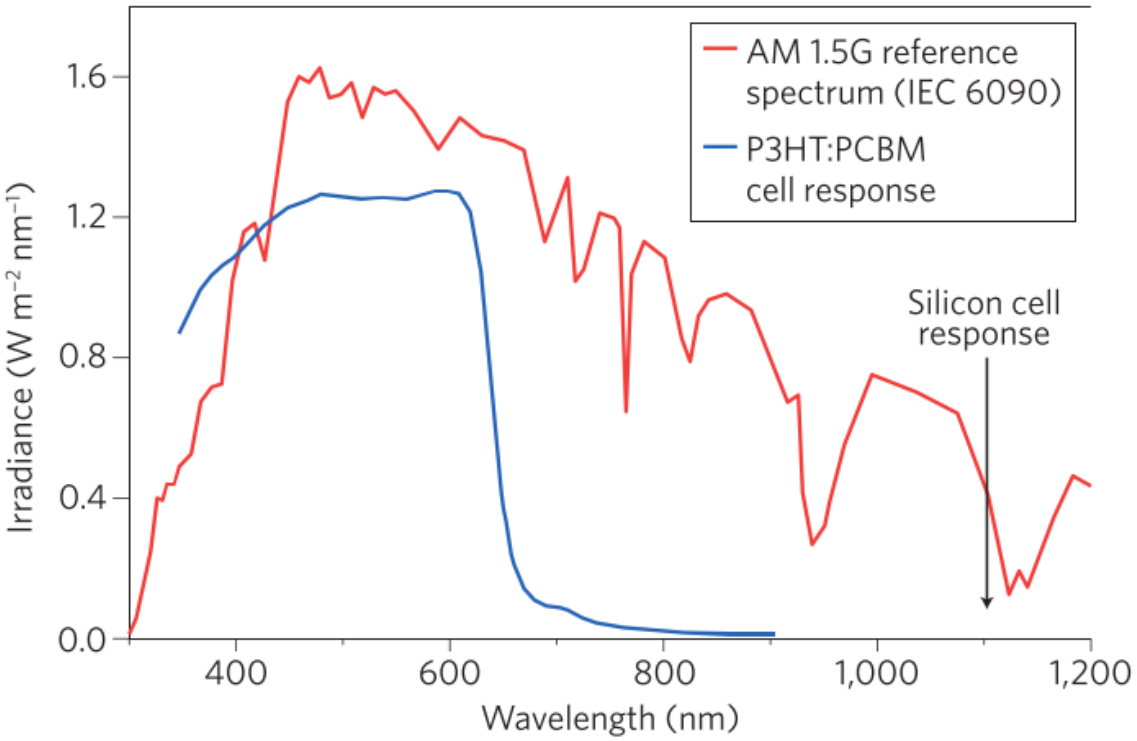

Figure 2.2. AM1.5G standard spectra compared to a solar cell with P3HT:PCBM.[7]

2.2 Conjugated Polymers

Traditional bulk polymers are used as effective insulators, e.g. in high-voltage cable applications. However, when the chemical structure of the polymer has alternating double bonds in the main chain, this changes. The discovery and development of conducting polymers started with Nobel price winners Alan MacDiarmid, Alan J. Heeger and Hideki Shirakawa in 1977.[14] Their work concerned iodine doped polyethyne, which can be considered the simplest conjugated polymer possible and consists of linear backbone with alternating single- and double bonds, sp^2-hybridized carbon atoms, seen in figure 2.3. Poly(p-phenylene vinylene) is a slightly more complex polymer, which also has an aromatic phenyl ring. The last polymer is polythiophene,

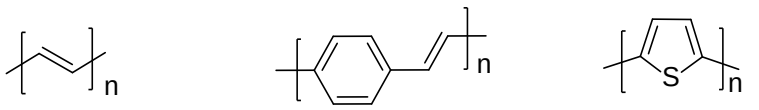

Polyethyne Poly(p-phenylene vinylene) Polythiophene

Figure 2.3. Three simple conjugated polymers.

Since conjugated polymers are not conducting in the ground state like metals, they are semiconductors. They have a band gap; an energy gap which needs to be overcome for electronic conductivity. Conjugated systems have empty π-orbitals above and below the plane of the molecule that can overlap. This means an electron excited from the ground state will enter a delocalized state where it can be transported away, leading to electrical conductivity. The band gap is central to the photovoltaic properties of a polymer. When the polymer is hit by a photon of an energy identical or higher to the band gap, an electron can be excited.

The third polymer in figure 2.3 is polythiophene, a five membered ring with a sulfur atom. Poly-3-hexyl thiophene (P3HT) is a polymer based on the polythiophene backbone, which is still commonly seen in modern applications. The large band gap energy needed to be overcome means only high-energy photons of wavelengths around 650 nm and below are absorbed. This can be seen in figure 2.2, where the absorption spectra for P3HT blended with Phenyl-C61-butyric acid methyl ester (PCBM) is compared to the solar spectra. This means that less than half of all photons striking this solar cell can even potentially be converted into electrical energy.

To improve the organic solar cell, a smaller band gap is required. The most prominent method to accomplish this is by combining electron rich and electron poor moieties in the polymer. Since the highest occupied molecular orbital (HOMO) will tend to be localized on the electron rich moieties and the lowest unoccupied molecular orbital (LUMO) will be localized on the electron pool moieties, the band gap will be closer to the difference in the high HOMO and the low LUMO of respective groups.[15] This way, a far lower band gap is achieved.

2.4 Polymer Solar Cells

Over the last few decades, the advancement of organic photovoltaic devices has been dramatic. One drastic improvement on the previously mediocre performances of organic photovoltaics came in 1995 when the bulk heterojunction (BHJ) was introduced.[16] Instead of bilayer devices, the interface between electron donating polymers and electron accepting fullerenes was drastically increased by intermixing of the phases. This resulted in a record power conversion efficiency (PCE) of 2.9%. Since then the development has been drastic and regularly exceed 11% with a recent publication showing above 13% efficiency for single junction devices.[17-20] One problem today, however, is the toxic nature of the most commonly used processing solvents such as chloroform and dichlorobenzene.[21] While they contribute little to the overall energy consumption in device production, in order to be called a green technology, they should

be replaced whenever possible.[2] In order to improve solubility in less harmful solvents, a variety of methods are employed to alter the solubility of conjugated polymers, with the end goal of making polymers suitable for printing from completely green solvents such as ethanol or ethanol/water-mixtures. There are many problems with this approach however. A major hurdle is the multi-layer structure of the organic solar cell. Sequential processing of the layers is needed, and it is important that the previous layer remains stable when subsequent layers are deposited on top,[21] or the device will have large current leakage and most likely fail completely.

The basic structure of a polymer solar cell For a polymer solar cell (PSC) to function, there are a few basic components needed. In the most basic shape, a solar cell consist of the following: A substrate, electrodes and an active layer. The substrate is often glass, or in printed applications PET-plastic. The cathode and anode transport electrons and holes, respectively. One of these needs to be transparent, so the photons can reach the active layer. The active layer is where the current is generated. In PSCs, this is a BHJ system with electron donating and electron accepting phases. To make sure there is no current leakage it is also beneficial to have interfacial layers in between the electrodes and active layer. This can also serve the purpose of tuning the work-function of the metal electrodes, to increase the contact and wettability to make sure a good film can be formed.

What governs how much energy a solar cell can produce depends on several factors. In simple terms, it depends on how much incoming light there is, and how much of it can be converted into electrical energy.[22] The PCE of a solar cell produces is described by:

$$PCE = \frac{J_{max}V_{max}}{P_{inc}} = FF\frac{J_{SC}V_{OC}}{P_{inc}}$$

Where J_{max} and V_{max} are the maximum values of the current and voltage and P_{inc} is the incident power density. J_{SC} is the short-circuit current, which can be said to depend on factors such as absorption, exciton diffusion, exciton dissociation into free charge carriers, charge transport and charge collection.[22] V_{OC} is the open-circuit voltage, which is mainly a function of the difference between electron donor HOMO and electron acceptor LUMO, i.e. the band gap. The fill factor (FF) is a function of the V_{OC} and the ideality factor of the diode.[23] This can be described as the "squareness" of the *J-V* curve. The closer to 1 the better, but typical values can be between 0.5-0.7. These factors are illustrated in the *J-V* diagram in figure 2.4.

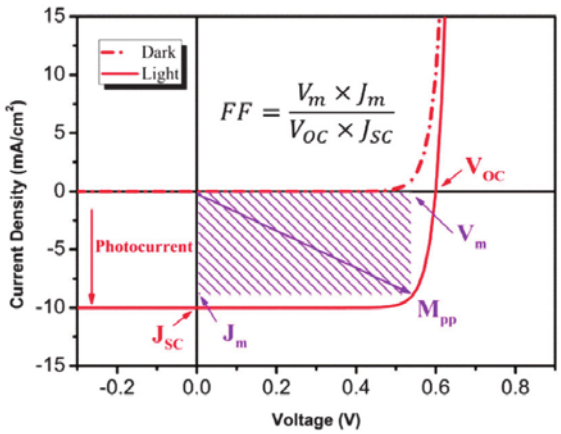

Figure 2.4. J-V curve where important factors are marked. The gray square illustrates the FF and the maximum power output is given by the square $J_m V_m$.[23]

2.5 Synthesis of Conjugated Polymers

Due to the commonly used donor-acceptor (D-A)-motif, the most commonly employed methods of synthesizing conjugated polymers for solar cells include having two bifunctional monomers, and using a palladium catalyzed reaction, often Stille Cross Coupling Polymerization or Suzuki Cross Coupling polymerization. These methods are both step-growth processes, which means they need to have a very high degree of polymerization to reach high molecular weight polymers. This, in turn, means the monomer purity and molar ratio needs to be highly accurate.[24]

Since the goal is often the highest achievable molecular weight when performing these polymerizations, there is a degree of superstition present in many polymer chemists. However, they are not necessarily very complicated. The two monomers are weighed up as precisely as possible, along with palladium catalyst and ligands. These are then put in a dry reaction vessel, dissolved in anhydrous, degassed solvent. In our case, often toluene. This is then heated under inert atmosphere with vigorous stirring until judged finished. This can be judged from solution viscosity of precipitation test, both highly dependent on experience. The polymer is then precipitated from a non-solvent, such as methanol. The solids are then filtered into a soxhlet thimble, after which several steps of solvent extractions take place. They can be used both to clean the polymer and to separate different molecular weight fractions. Most of the polymers are extracted with chloroform. After this step, the polymer is purified over a short silica gel column and then once again precipitated from methanol, filtered, dried and collected.

2.6 Characterization of Conjugated Polymers

There are a wide variety of ways to characterize polymers. Some of the most common methods are presented briefly below. Since conjugated polymers for organic electronics serve completely different purposes than common bulk polymers like polystyrene and polyethylene, their characterization differs accordingly. More focus is put on electrochemical- and optical properties and less on mechanical properties.

Gel Permeation Chromatography GPC

Gel permeation chromatography (GPC) is a very common way to study the molecular weight of polymers, and can give information about weight average-(M_w) and number-average molecular weight (M_n) as well as the polydispersity index (PDI) of the polymer.[24] It is a variety of size-exclusion chromatography where molecule size determines the speed at which they can travel through a column. In our case, porous beads of crosslinked polystyrene is used as stationary phase and the mobile phase is 1,2,4-trichloro benzene heated to 150 °C.. Because of diffusion in and out of the pores, smaller molecules travel slower.

UV-Vis Spectroscopy

To study the optical properties of polymers, the common way is to use spectroscopy to study absorption spectra in either solution or film. In its most basic form, UV-Vis spectroscopy is very simple. A light of known intensity and wavelength passes through a sample of known length. For simplicity, in solution this is usually 1 cm. The detector detects how much of the light is absorbed by the sample, and the fraction I/I_0 is calculated. This uses the Beer-Lambert law.[25]

$$A = log_{10}\left(\frac{I_0}{I}\right) = \varepsilon cl$$

A is the absorption, I_0 incident light and I light transmitted through the sample, ε the absorption coefficient, c the concentration and l is the length. Often, the spectra is normalized, in order to see the shape and absorption maximum, without taking the absorption coefficient into consideration. When the absorption is used to calculate the optical band gap, the onset of absorption is used.

Electrochemistry

In order to study the electrochemical properties of polymers, the most common methods are cyclic voltammetry (CV) and square wave voltammetry (SWV).[26-28] These can be measured using an electrochemical workstation. The polymer is deposited onto a platinum electrode, dipped into an electrolyte solution with a counter electrode and a silver (Ag/Ag^+) reference electrode. A potential is applied over the sample and the current is measured. This is done for both positive and negative potential, and a curve of current over potential is received. For SWV the oxidation and reduction are calculated from the maximum and minimum peak currents,[28] while the onset of oxidation or reduction is used in CV.[26]

Thermogravimetric analysis

A common method to study thermal stability in a polymer is thermogravimetric analysis (TGA). This method uses a finely calibrated balance which can be heated. The weight transitions are then registered as a function of temperature. The temperature is slowly increased, but the degradation is still somewhat time dependent, so a thermal transition temperature is calculated from onset temperature. Here the temperature was increased from 25 °C to 550 °C using a speed of 10 °C per minute.

Atomic Force Microscopy

Atomic force microscopy (AFM) is a surface sensitive method which can be used to analyze the morphology of surfaces down to the atomic level. AFM uses a cantilever with an extremely fine tip which can tap a surface. By focusing on the back of the cantilever with a laser, which is constantly monitored, it is possible to sequentially scan a surface and gain information about the topology of it.

Contact Angle Measurements

By measuring the angle between a surface and a drop of deionized water, it is possible to measure the free energy of a surface.[29] This is a simple but effective method, where modern instruments automatically measure drop volumes and contact angles, enabling a larger sampling and statistical robustness. The surface free energy is directly related to the hydrophilicity/hydrophobicity which is important for the morphology at the interface in organic electronic application where thin layers of different surface energies are stacked.

3. Morphology Analysis by Transmission Electron Microscopy

Transmission electron microscopy (TEM) is very powerful method to study the bulk of a sample. TEM makes use of the short wavelength of electrons accelerated to high speeds to visualize material properties. By comparison, the relatively large wavelength of photons in the visual range limit the maximum resolution to around 1 µm, while electron microscopy has theoretical resolutions of less than 1 Å, which means atomic resolution is achievable. In transmission electron microscopy the electron beam is transmitted through an extremely thin sample in the range of 100 nm. The electrons will interact with the atoms in the sample in several ways, generating signals that can be used to analyze the bulk properties.

TEM is very useful to analyze films of polymer:PCBM used in organic photovoltaics.[30] The bulk morphology of these blends directly affect the performance of devices which means surface sensitive methods such as AFM are less interesting.[30-31] Furthermore, TEM sample preparation can be very time consuming and tedious, depending on the sample. This is generally not the case for organic thin films from solar cells since they are of suitable thickness and can be spin coated on top of poly(3,4-ethylenedioxythiophene):polystyrene sulfonate (PEDOT:PSS) which is dissolved in water, leaving the active layer floating. The active layer thin film can then be deposited directly onto a TEM sample grid from the water and studied in the microscope. A disadvantage when used to study organic thin films, is that some of the power of the technique can be lost, since much of the sample consists of amorphous carbon with roughly the same electron scattering. This means sufficient contrast between phases of material can be hard to generate, leading to images of gray noise.[32]

In addition to common morphology analysis in organic photovoltaics, TEM has been used to study other parameters, such as time- and temperature dependent processes in the morphology, e.g. phase separation and PCBM crystallization.[33-36]

Morphology study from paper 1: Polymer $PC_{71}BM$ blends with donor polymers with ortho- or meta-substitution of alkyl chains on the IDTT segment.

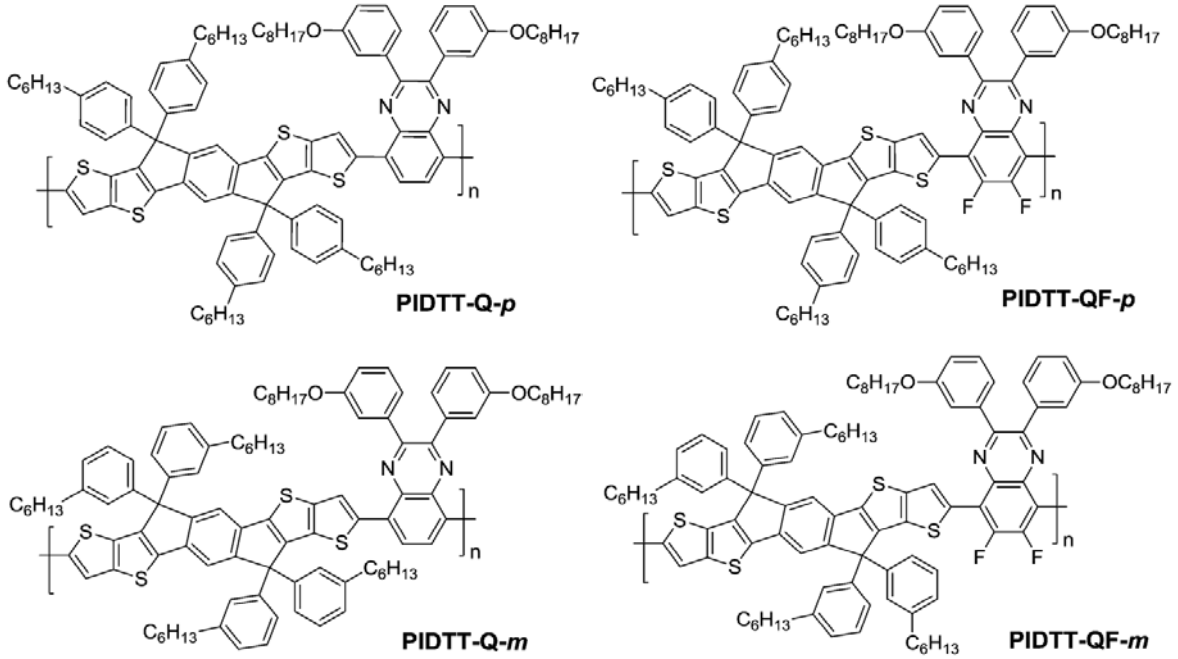

Figure 3.1. The four active layer donor polymers used in the study.

The primary goal here was to study the effect of changing the para-substituted phenyl pendants to meta-substitution, as well as to see if fluorination of the quinoxaline acceptor segment would positively affect device performance. The chemical composition of the polymers are shown in figure 3.1. The morphology was investigated using TEM and representative micrographs are shown in figure 3.2.

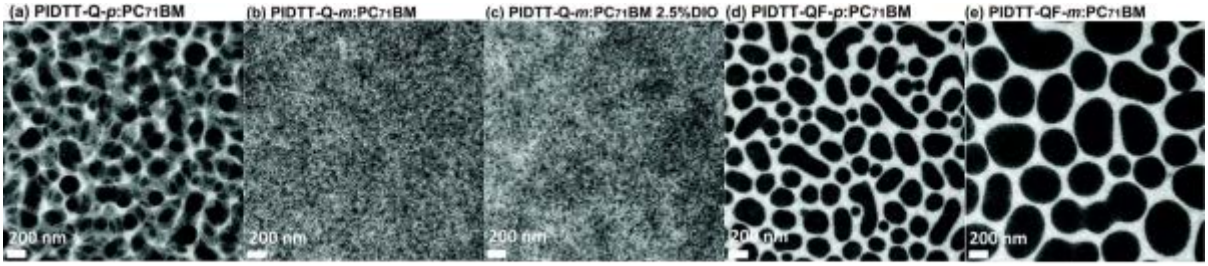

Figure 3.2. TEM bright field images of the four polymers in 1:4 ratio with $PC_{71}BM$.

For the two fluorinated polymers PIDTT-QF-p and PIDTT-QF-m large areas with very high electron scattering can be seen. These are attributed to extensive aggregation of $PC_{71}BM$, which has a higher scattering density than the polymer. Both of these polymers gave poor results in solar cell devices due to the large phase separation. When comparing PIDTT-Q-p and PIDTT-Q-m, a drastic effect on bulk morphology can be seen. For the para-substituted polymer, large polymer fabric can be seen, while the meta substituted polymer showed very fine morphology, but still continuous pathways of finely aggregated $PC_{71}BM$. This resulted in significantly

improved device performance, which was further improved when processed with trace amounts of diiodooctane (DIO). By density functional theory (DFT) calculation, the improved morphology of PIDTT-Q-m was ascribed to the para-substituted chains extended in either direction, while the meta-substituted chains tended to wrap around the polymer backbone, enabling more efficient stacking. These results are a good example of the power of TEM analysis of bulk morphology, which gives important information about device performance.

Morphology study from paper 2: Solar cells based on novel electron deficient unit PQD.

In this study, the new electron deficient block PQD was presented and used in four different copolymers. The donor-segments used were three varieties of BDT and one with a thiophene spacer. Their chemical compositions are shown in figure 3.3.

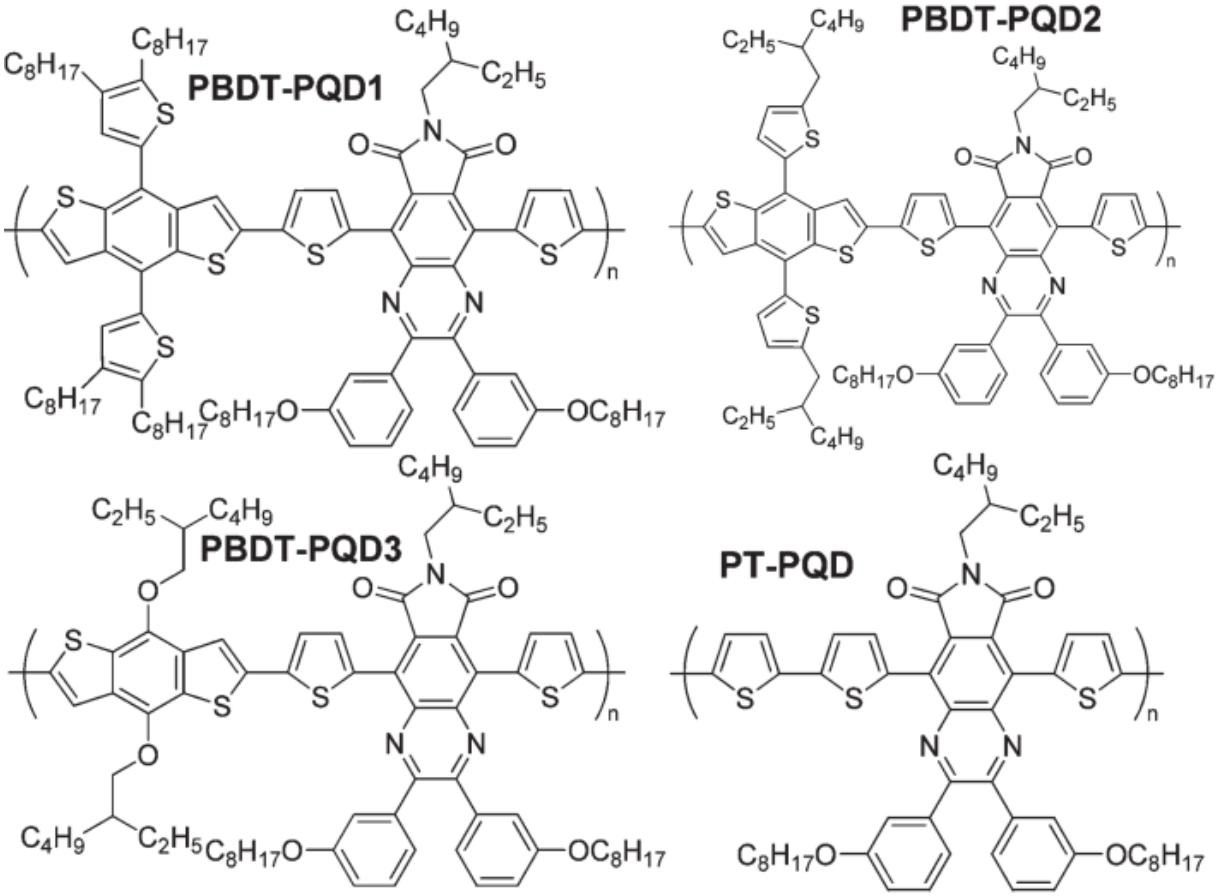

Figure 3.3. Chemical composition of the four novel polymers.

These polymers were tried in PSCs with $PC_{71}BM$ and the films were studied by bright field TEM. The resulting micrographs in figure 3.4 are a perfect example where TEM is not the optimal instrument.

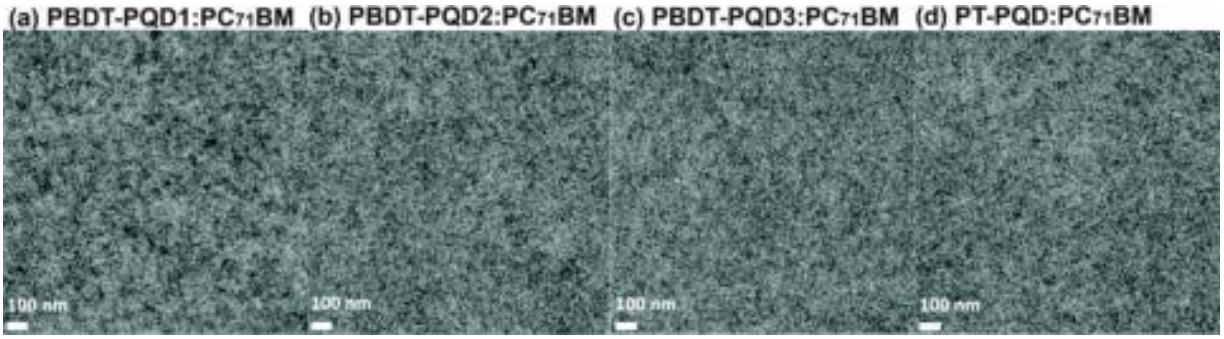

Figure 3.4. Bright field TEM micrographs of the four polymers in 1:3 blend with $PC_{71}BM$.

By first glance, the four images are close to identical. This is the result from highly intermixed blends where the individual phases are hard to make out and further study might be needed. As for the previous section, the darker areas are attributed to $PC_{71}BM$-richer areas and the light areas are polymer rich. There are likely no significantly pure domains here. The morphology for all four polymers are likely to be favorable for charge separation, since domains are close to the exciton diffusion length of around 10 nm in these materials. The four polymers had significant differences in photovoltaic performance, however it cannot be attributed to differences in morphology, as in the previous paper.

Morphology study from paper 3: A novel low band gap polymer which exhibits very low voltage loss in devices.

In this study a novel low band gap polymer is presented and used in PSCs with $PC_{71}BM$. The polymer, abbreviated PIDTT-TID is shares the meta-substituted IDTT block shown in figure 3.1, but with a new acceptor segment called TID. The chemical composition is shown in figure 3.5.

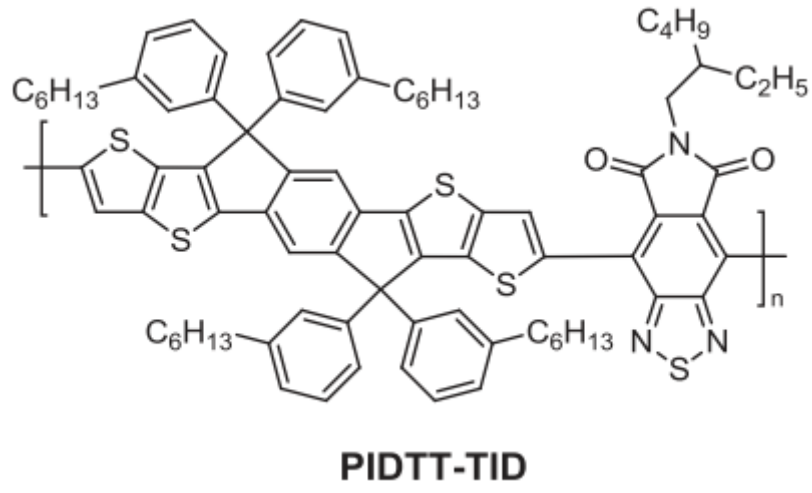

Figure 3.5. The novel low band gap polymer PIDTT-TID.

By comparison, this study consisted of only one donor polymer and instead the $PC_{71}BM$ content was varied and an optimum ratio of 1:3 or 1:3.5 was found, where both had similar performance. The micrographs from this study are shown in figure 3.6.

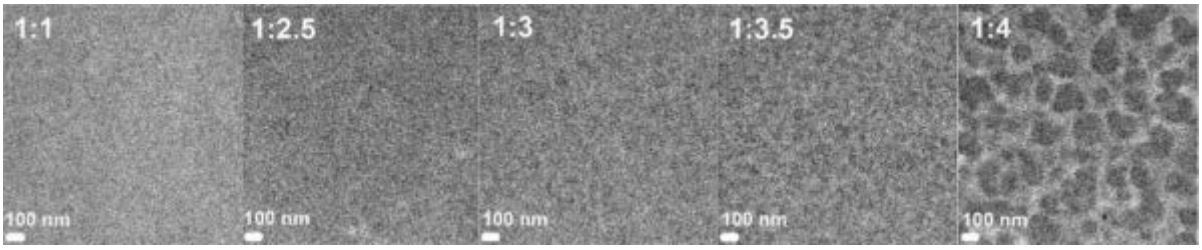

Figure 3.6. TEM bright field micrographs of PIDTT-TID:$PC_{71}BM$ with ratios from 1:1 to 1:4.

This study is interesting in when compared to the previous two studies, since the ratio of $PC_{71}BM$ is varied, instead of including different donor polymers. An obvious trend can be seen where the 1:1 ratio has extremely fine morphology, the phase separation increases gradually, until the 1:4 ratio shows large, phase separated regions similar to what was seen in figure 3.2. The morphology is not the only factor affecting the performance of a BHJ-film, but in this case it likely played a role. The optimal ratios were somewhere around 1:3 to 1:35, where the former had slightly higher J_{SC} but lower FF, giving identical total PCE of 6.7%. As the TEM-micrographs show, when going from 1:1 to 1:3, PCBM rich domains around 1-10 nm start forming. In the 1:1 case, the morphology might have been too fine to form large enough contionous domains for efficienty charge extraction.

4. Thermocleavable polymers

One way to modify the solubility of polymers is to include cleavable moieties that solubilize the polymer until toggled off by external stimuli. These stimuli can be many, such as heat, UV-light, acid or base.[37-48] Since solar cell devices are produced by sequential deposition of layers, any treatment after the active layer is at risk of leaving cleaved off compounds in the film. Generally, unwanted compounds containing ions or radicals will be very harmful for the stability and performance of a solar cell.[49] One simple protecting group called *tert-butyloxycarbonyl* (BOC), however, produces only gaseous products after cleaving.[43] This means that the solar cell can be heat treated after deposition of the active layer, leading to an insoluble active layer with increased long term stability.[38]

Previous studies have mostly focused on thiophenes.[38, 40-42, 45-46] A few have made use of the facile synthesis using BOC-protection of amines, instead of esterification from alcohols and carboxylic esters. This method has been used for some electron-accepting units such as diketopyrrolopyrrole (DPP) and isoindigo (II).[43-44, 50] In order to produce solvent resistant polymers for solar cells, based on conventional solar cell materials, the II moiety was chosen as a suitable candidate. In order to study the properties of the BOC-protected indigo compared to conventional branched alkyl chain one, a series of copolymers and pure polymers were produced and the solubility and thermal stability was investigated. The chemical composition of the polymers are illustrated in figure 4.1.

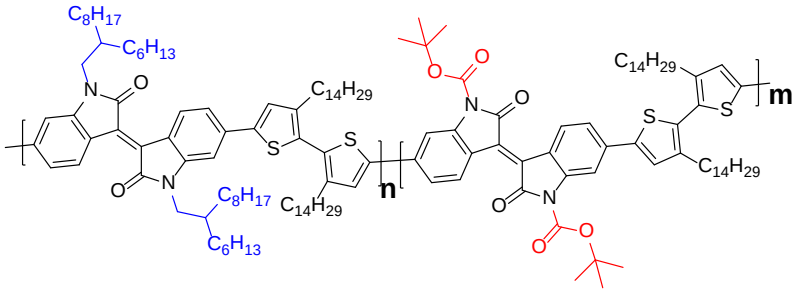

P2TI:	**n=1, m=0**
P2TI-BOC10:	**n=0.9, m=0.1**
P2TI-BOC20:	**n=0.8, m=0.2**
P2TI-BOC50:	**n=0.5, m=0.5**
P2TI-BOC:	**n=0, m=1**

Figure 4.1. Chemical composition of the five polymers.

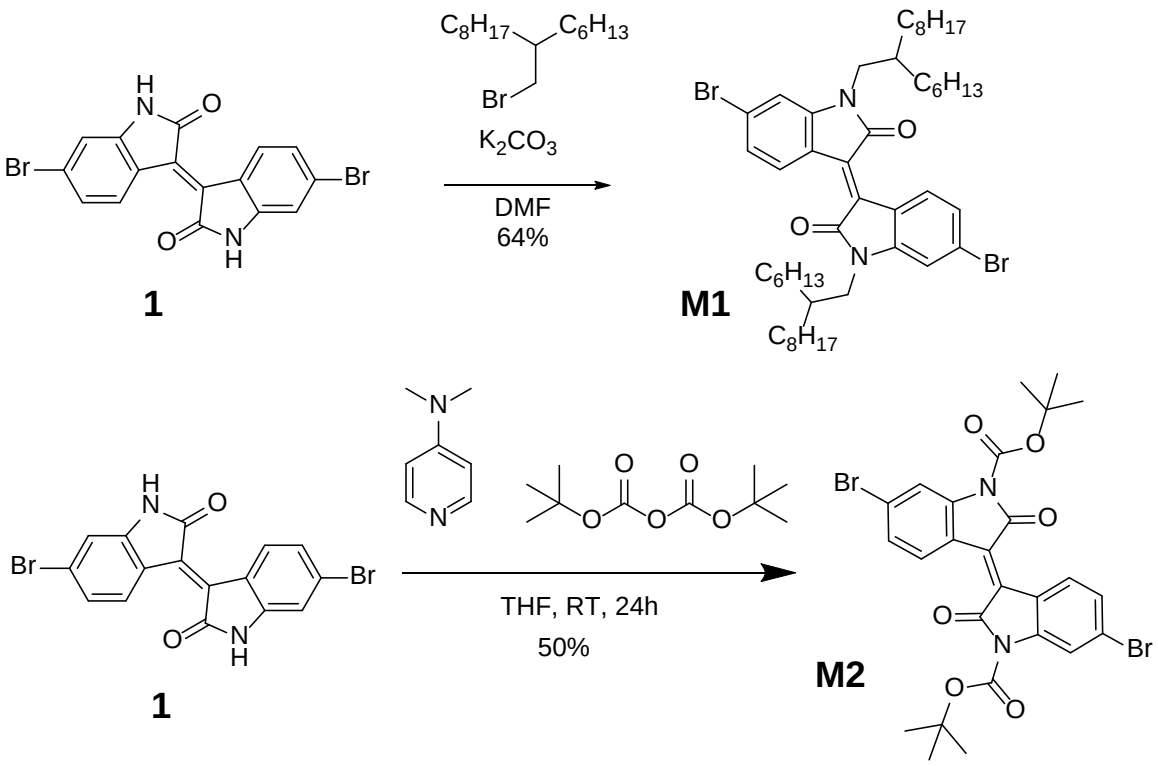

Figure 4.2. Monomer synthesis.

The synthesis of the monomers in this study were quite simple one step reactions from the basic, dibrominated isoindigo moiety. The reaction schemes are shown in figure 4.2. For **M1** it includes a base-catalyzed alkylation reaction, taking place in dimethylformamide (DMF). Due to the mirrored structure with two reactive sites, and relatively slow reaction rate, it is important with proper purification after alkylating. Monoalkylated isoindigo byproduct is always present, but the big difference in polarity makes column chromatography a suitable way to purify the monomer. The reaction yield can be anywhere from good to excellent.

For **M2**, the reaction is also a one-step reaction based on the work of Nguyen *et al* where DPP was BOC-protected in a similar position. In this case, the dimethylamino pyridine (DMAP) base catalyst is used to cleave a di-tert-butyl dicarbonate molecule and attach to the secondary amine in the isoindigo molecule. This reaction is commonly used to protect reactive amines in subsequent steps, thus the intention is to have a simple, high yielding reaction that is easy to revert after the protection is not needed anymore. The formed tertiary butyloxycarbonyl product is sensitive to both thermal energy as well as acid. Due to this instability, an ordinary silica column is unsuitable as it is a bit acidic. This means the compound is unprotected and binds to the silica. It was instead purified on a short column of neutral aluminium oxide. The yield in this case was unsatisfactory at around 50%, but should be possible to increase with some heating or longer reaction time.

For this study, two D-A alternating polymers and three random copolymers were synthesized. They were all made using stille cross coupling polymerization and a reaction scheme can be seen in figure 4.3.

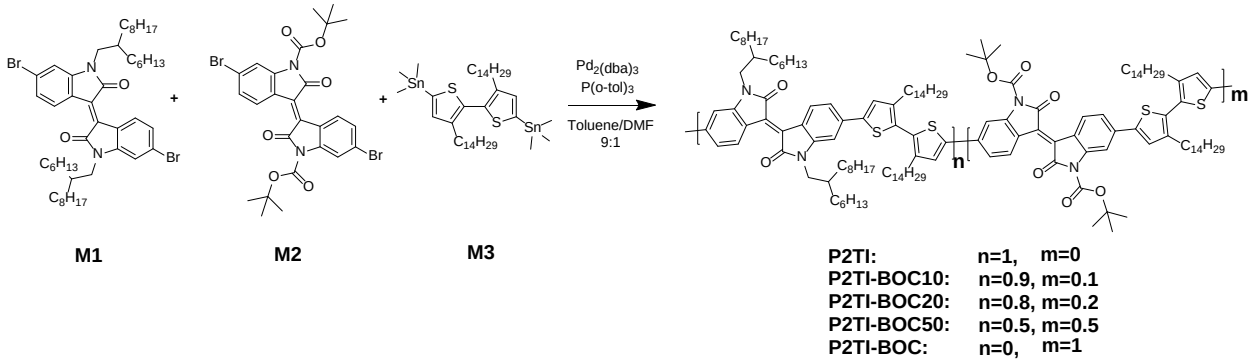

Figure 4.3. Synthesis of thermocleavable sidechain containing polymers.

P2TI contains pure conventional branched alkyl chain monomer while P2TI-BOC contains pure thermocleavable side chain monomer. The three polymers P2TI-BOC50, 20 and 21 are copolymers with varying amounts of thermocleavable monomers. The synthesis procedure was identical, except for the monomer amounts. The third monomer is a bithiophene with very long sidechains, namely n-tetradecyl chains containing fourteen carbons. This was intentionally chosen, since without the much longer branched sidechain on isoindigo, the polymer was judged to have too low solubility without it. It also serves the purpose of clearly showing that a solvent resisting polymer after cleavage would depend on hydrogen bonding and not just lack of sidechains.

The polymerization reactions took place in round bottom flasks, carefully dried, in anhydrous solvent, under nitrogen atmosphere for up to 72 hours. Due to the somewhat unstable nature of the cleavable side chain, the reaction temperature was 60 °C. Generally these reactions are performed at 80 °C or higher. For purification, the polymers were precipitated from methanol, filtered into a soxhlet thimble, washed in a sixhlet extractor with petroleum ether, diethyl ether, acetone and then extracted with chloroform. They were then pushed through a short column of neutral aluminium oxide to get rid of residual traces of catalysts and other impurities, which can severely damage device performance, and then reprecipitated from methanol. They were then filtered on very fine PTFE-filters and dried at 40 °C in a vacuum oven.

The polymers' molecular weight was measured by GPC and presented in table 4.1, showing acceptable molecular weights for all but P2TI-BOC50. This was later judged to be a miscalculation of monomer ratios, which once again highlights the importance of accurate ratios for polymerization reactions.

Table 4.1. Molecular weights of the polymers.

Polymer	M_n (kDa)	M_w (kDa)	PDI
P2TI	42	108	2.6
P2TI-BOC	41	108	2.7
P2TI-BOC50	6	13	2.0
P2TI-BOC20	22	51	2.3
P2TI-BOC10	30	70	2.3

The optical properties were measured in chloroform solution, in film, and in annealed film after 10 min at 200 °C. The results are shown in figure 4.4.

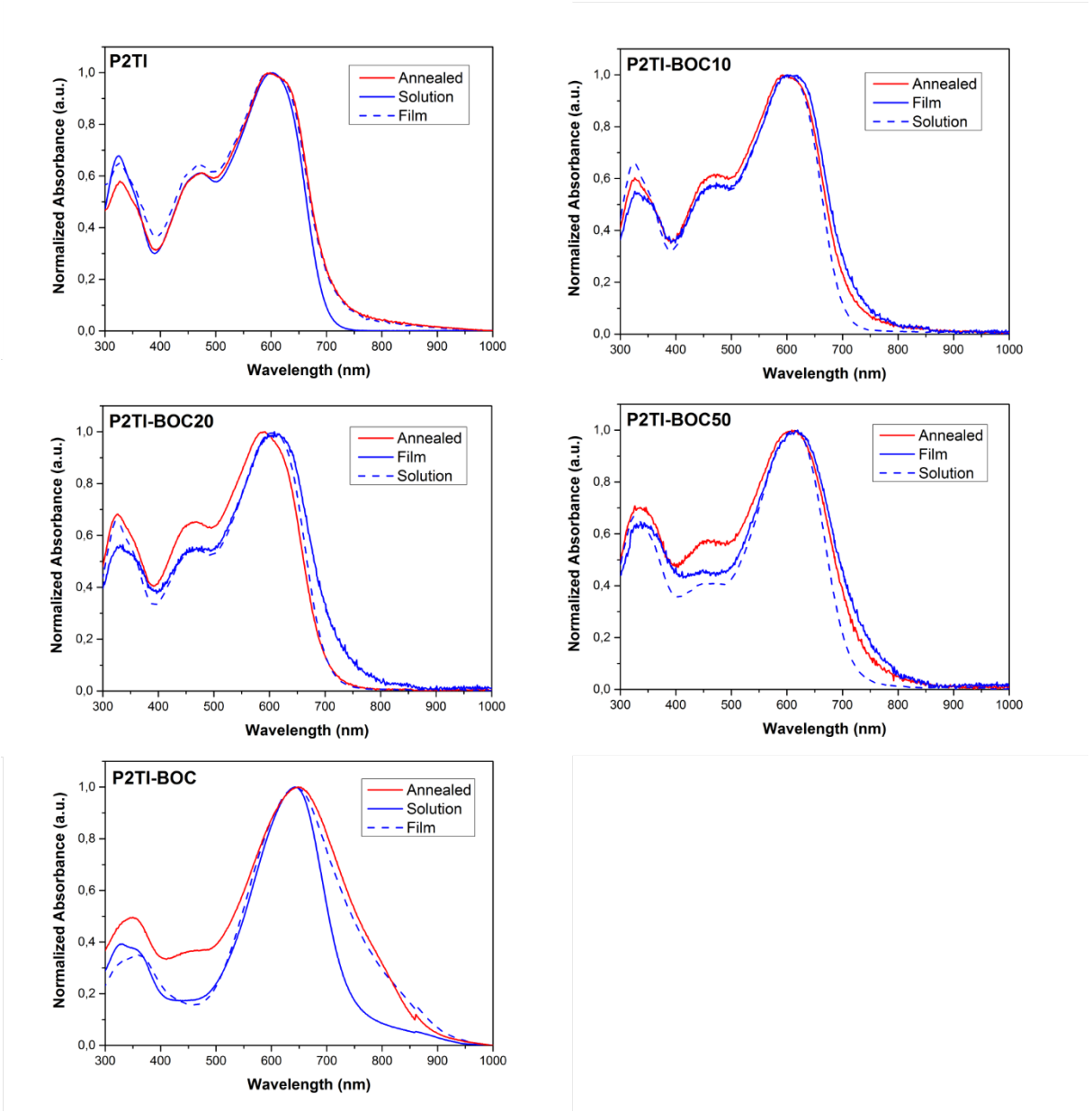

Figure 4.4. UV-Vis spectra of the five polymers in solution, film and annealed films.

It is common to see a red shift in absorption when going from solution to film, however no such transition is seen here. This indicates that the inter-chain interaction is weak, possibly due to steric hindrance from the side chains. There is a small red shift going from alkyl to t-BOC side chain, which can be explained by the increased electron deficiency of the isoindigo group. This leads to a deeper LUMO, giving a smaller band gap. The interesting shift takes place when going from film to annealed film. When the sidechain cleaves off, there is a noticeable increase in low wavelength absorption and notably a new absorption maximum below the two peaks. To study electrochemical properties, cyclic voltammetry was used. The results are shown in figure 4.5.

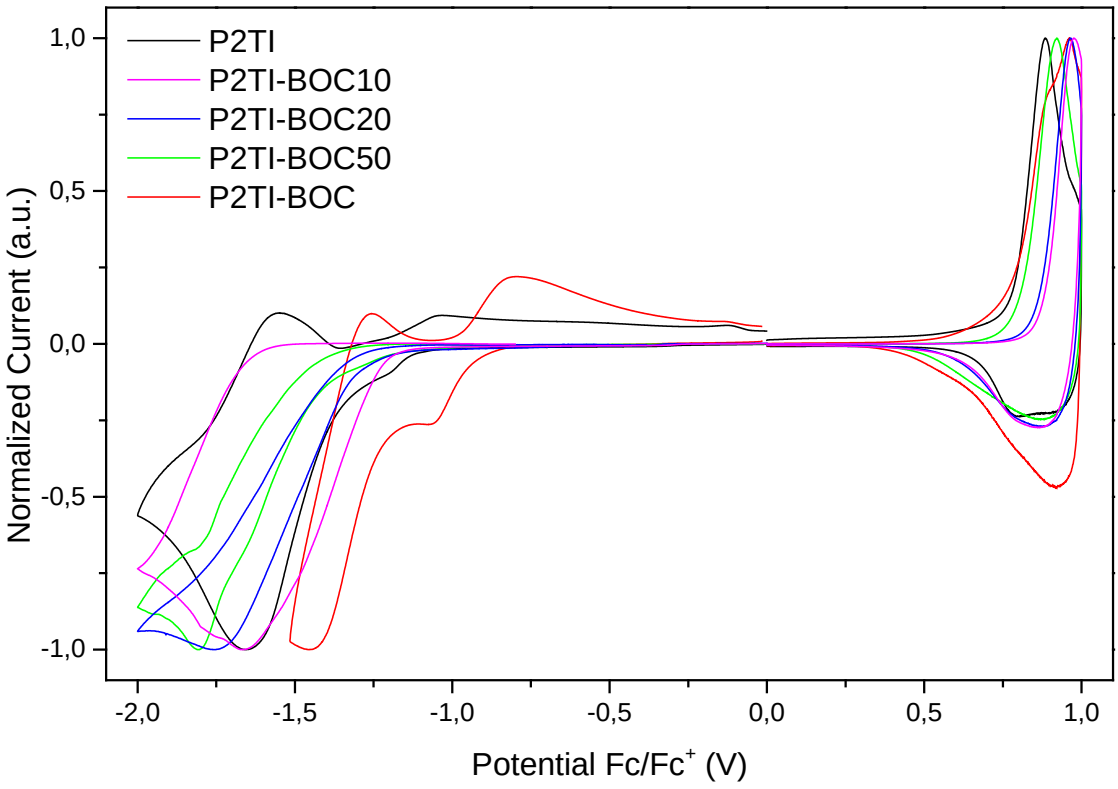

Figure 4.5. Cyclic voltammogrammes for the five polymers showing oxidation and reduction peaks for the two polymers.

Both electrochemical and optical properties are summarized in table 4.4.

Table 4.4. Electrochemical- and optical properties determined by CV and UV-Vis.

	electrochemistry			absorption			
				solution	film		
polymer	HOMO (eV)	LUMO (eV)	E_g^{ec} (eV)[c]	λ_{max}[a] (nm)	λ_{max}[b] (nm)	λ_{onset} (nm)	E_g^{opt} (eV)[d]
P2TI	–5.9	–3.8	2.2	600	596	704	1.8
P2TI-BOC10	–6.0	–3.9	2.1	607	601	705	1.8
P2TI-BOC20	–6.0	–3.8	2.2	608	605	706	1.8
P2TI-BOC50	–5.9	–3.7	2.2	615	610	709	1.8
P2TI-BOC	–5.9	–4.0	2.0	642	642	819	1.5

[a)]Electrochemical band gap; [b)]Absorption maximum in chloroform solution; c)Absorption maximum in film; [d] Optical band gap

To verify cleavage of the t-BOC group, thermogravimetric analysis (TGA) was performed for all five polymers and is shown in figure 4.6.

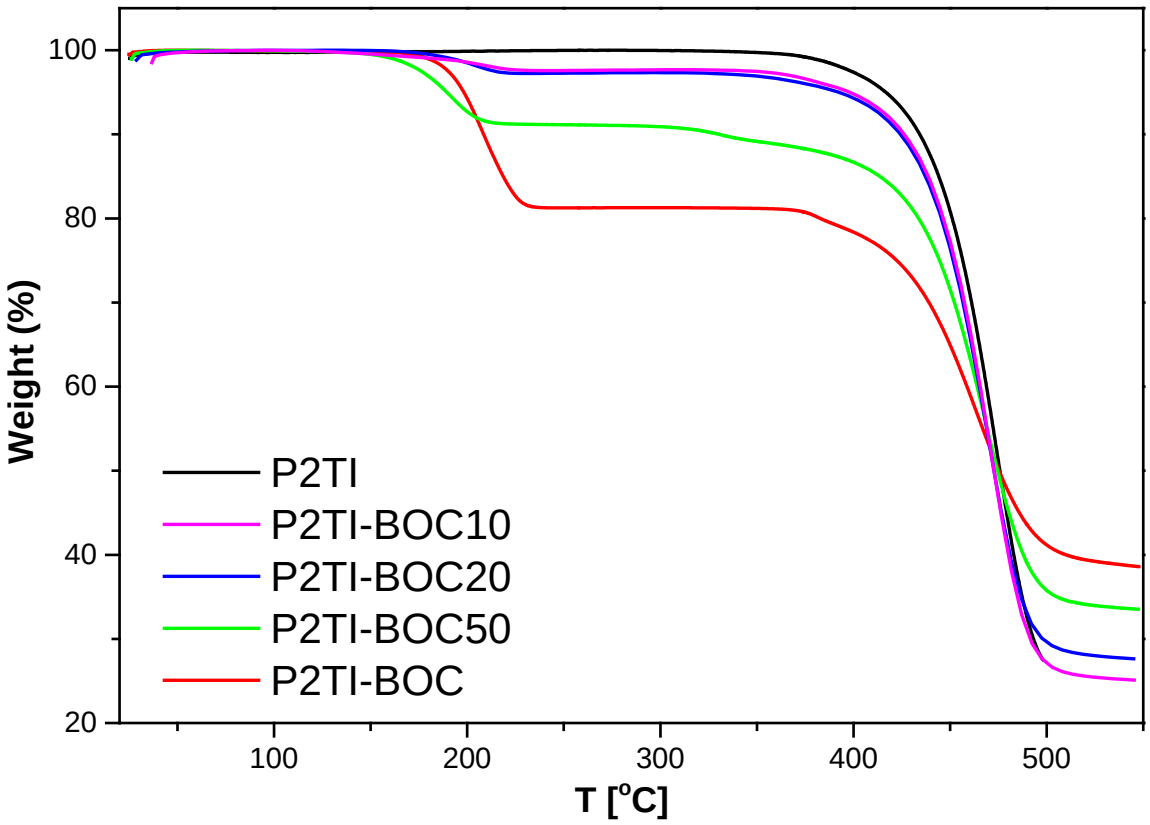

Figure 4.6. TGA analysis of the five polymers, showing onset of degradation below 200 °C for the t-BOC containing polymers.

The TGA analysis clearly shows that the polymer without cleavable sidechain stays stable to around 400 °C while the others have a mass-loss that corresponds to complete decarboxylation. Based on previous publications, this result was expected. Interesting to note is also that the thermocleavable polymers stabilize on higher weight-% at above 500 °C. The values from the TGA measurements, compared with theoretical weight losses are displayed in table 4.5.

Table 4.5. Molecular weights and thermal degradation of copolymers

	molecular weight			thermal degradation			
polymer	M_n (kDa)	M_w (kDa)	PDI	T_d^{1a} (°C)	T_d^{2a} (°C)	weight loss[b] (%)	weight loss[c] (%)
P2TI	42	108	2.6	-	434	-	-
P2TI-BOC10	30	70	2.3	183	434	1.6	2.4
P2TI-BOC20	22	51	2.3	182	434	3.3	2.8
P2TI-BOC50	6	13	2.0	170	427	8.8	8.8
P2TI-BOC	41	108	2.7	189	422	19.6	18.7

[a)] T_d^1 = Temperature of the first decomposition; T_d^2 = Temperature of the second decomposition; [b)] Theoretical weight loss of the t-BOC side chain; [c)] Experimental weight loss observed

A rudimentary solubility study using films were also performed. The polymers were spin coated onto glass slides, annealed and then submerged in chloroform. It turns out P2TI was still completely soluble, which is to be expected. P2TI-BOC was completely insoluble after cleaving, and the copolymers were somewhat soluble. To further study the effect of this stabilization, a morphological study for a polymer:PCBM blend using TEM and AFM was performed. Figure 4.7 shows example micrographs of the films in TEM and figure 4.8 is the AFM.

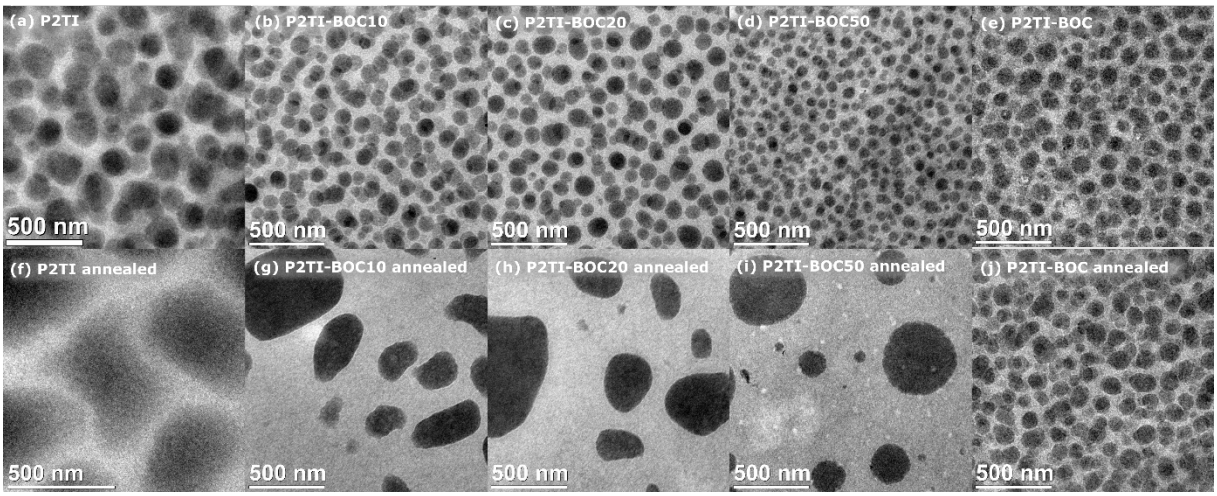

Figure 4.7. TEM bright-field micrographs of the five polymers in 1:1 blend with $PC_{60}BM$. (a-e)Without thermal annealing (f-j) with thermal annealing.

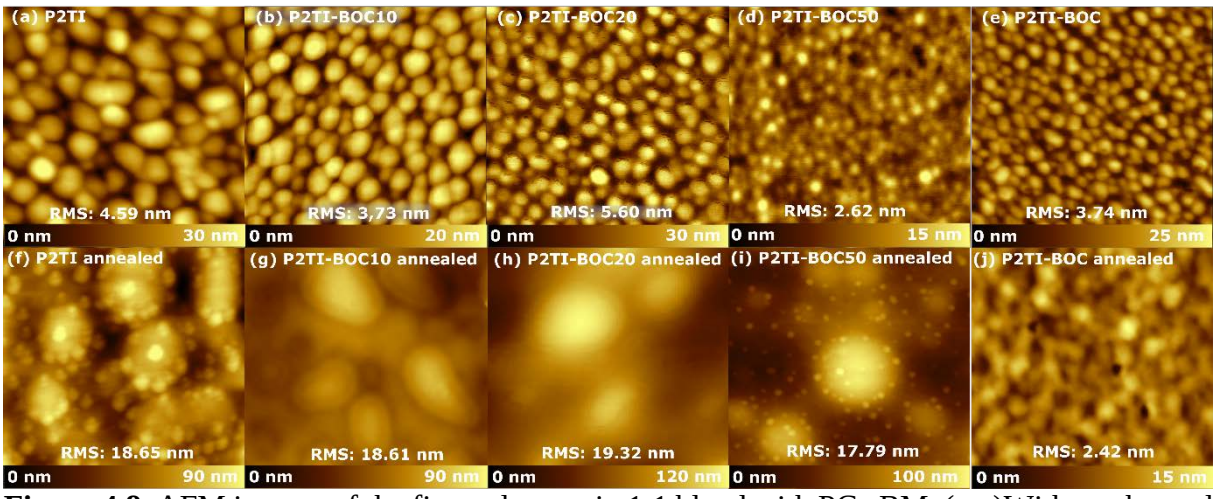

Figure 4.8. AFM images of the five polymers in 1:1 blend with $PC_{60}BM$. (a-e)Without thermal annealing (f-j) with thermal annealing.

When exposed to high temperatures, the sensitive morphology of these blends is expected to coarsen and large crystallites of PCBM form. This trend is clearly seen for P2TI-BOC50-P2TI-BOC10, where huge crystals form. For P2TI-BOC, however, this trend is not observed at all. This indicates a stabilized morphology. If not for this effect, the high annealing temperature

needed would be impossible to utilize in solar cells, since the performance is greatly dependent on film morphology.

5. Conjugated Cathode Interlayers for All-Polymer Solar Cells

The polymers presented in section 3 of this thesis were D-A-polymer with diethylamine pendant groups. The use for these polymers is more commonly as interfacial layers between active layer and cathode. In this position, they can be utilized in extremely thin layers, around 5 nm, which means the harmful effects of their hole-trapping amine functions doesn't affect the devices significantly. Used in this way, they serve several important functions.[51-53] Primarily, they can modify the work function of the electrode metal, tuning it more finely to the active layer energy levels. They have also been proven to n-dope the PCBM-acceptor of the BHJ, increasing their electron transport and reducing interfacial resistance. They serve as an compatibilizer, tuning the wettability of the two faces which affects the interfacial morphology. They also serve as a diffusion barrier, stopping metal ions from diffusing into the active layer where they would harm the device performance.

Since one of the main function of these polymers is to dope fullerenes and organic solar cell research has focused more and more on fullerene-free solar cells, the question is what purpose they can serve in an all-PSC. The expected increase in performance is lower, even if the important work function tuning would still be present. In order to study if conventional conjugated cathode interlayers design is still valid, we present a series of four polymers used as cathode interfacial material in all-PCSs. The chemical composition of the polymers used in this study are shown in figure 5.1 where the backbones are colored blue, and the pendant groups are red.

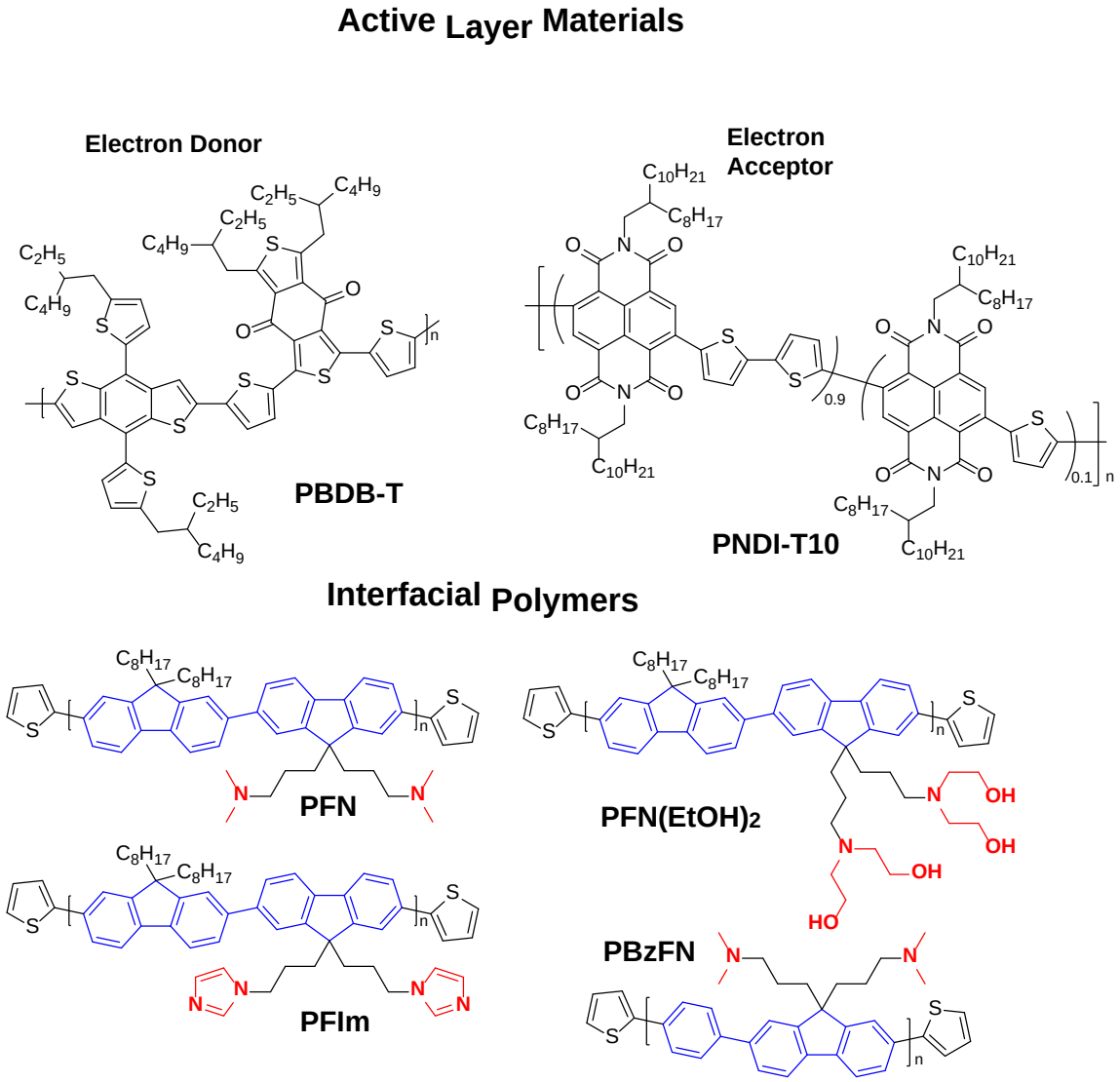

Figure 5.1. Chemical structures of the active layer polymers (Top) and interfacial polymers (Bottom).

The monomers used to produce these polymers were purchased and used without further purifications, except for the monomer **M1** which was made in a one-step reaction from 2,7-dibromo-9H-fluorene. The polymers were synthesized in a similar fashion to previously presented polymers, with the addition of a post-polymerization reaction step for PFN, PFN(EtOH)2 and PFIm. These three polymers were synthesized from a precursor polymer called PFBr. The synthesis of these polymers and the monomer synthesis are illustrated in figures 5.2.

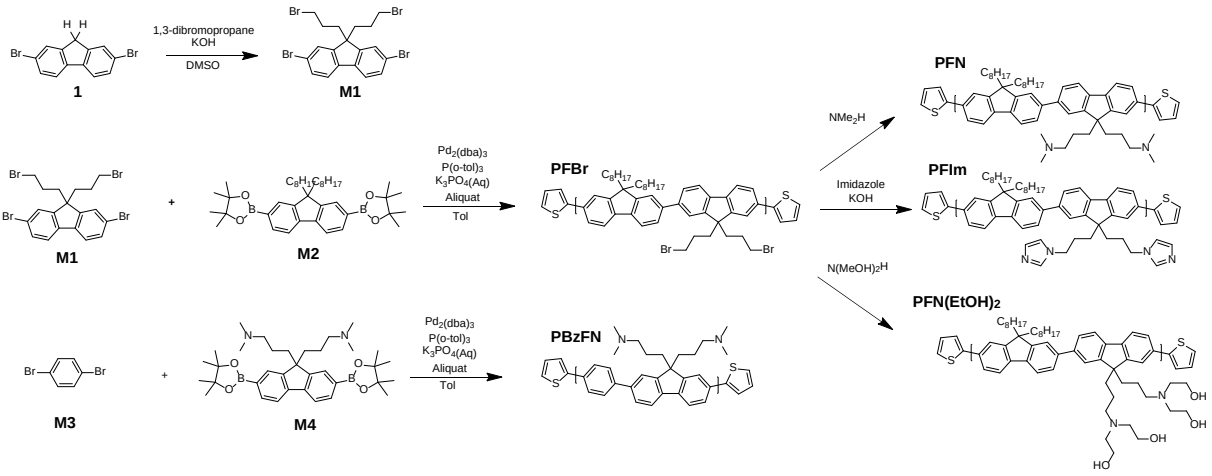

Figure 5.2. Synthesis of the four interlayer polymers.

Since the primary focus in this work was the interfacial layers, they were characterized extensively. Their energy levels were determined by CV and their optical properties by UV-Vis and compared to that of the precursor polymer PFBr. These results are summarized in table 5.1.

Table 5.1. Electrochemical and optical properties

	electrochemistry			absorption			
				solution		film	
polymer	HOMO (eV)	LUMO (eV)	E_g^{ec} (eV)	λ_{max} [b] (nm)	λ_{max} [c] (nm)	λ_{onset} (nm)	E_g^{opt} (eV)[d]
PBDB-T	–5.63	–3.34	2.29	616	578	678	1.83
PNDI-T10	–6.36	–4.02	2.31	639	688	798	1.55
PFBr	–6.09	–2.38	3.71	381	377	420	2.95
PFN	–6.02	–2.44	3.58	389	385	425	2.92
$PFN(EtOH)_2$	–5.83	–2.52	3.44	381	386	424	2.92
PFIm	–6.14	–2.45	3.69	390	381	424	2.92
PBzFN	–5.94	–2.57	3.37	375	370	415	2.99

[a]Electrochemical band gap; [b]Absorption maximum in chloroform solution; [c]Absorption maximum in film; [d]Optical band gap.

All four of the interlayer polymers show very similar properties to the precursor polymer PFBr, which is not strange considering their backbone similarities. The conjugated backbone is the component that governs these properties. While PBzFN differs a bit, it is still a series of phenyl-rings, giving a twisted backbone structure from the high dihedral angle.[54]

The polymers were used in all-PCS devices with conventional structure (ITO/PEDOT:PSS(40 nm)/active layer (~90 nm)/Interlayer/Al(90 nm)). The interfacial layer polymers (0.2 mg/mL) were spin-coated from an acetic acid: methanol solution (0.5%, v/v) onto active layers. PFN and PBzFN showed good solubility, while PFIm and PFN(EtOH)$_2$ had limited solubility and had to be filtered before spin-coating. The photovoltaic parameters are summarized in table 5.2 and the *J*–*V* curves and EQE curves are depicted in figure 5.3.The performance of devices with bare Al-electrodes was expectedly very low. The low performance of these devices can be explained by the lack of work-function tuning of the electrode, as well as inefficient charge extraction due to high contact resistance. This is clearly visualized in the *J*-*V*-curve where significant losses in both J_{sc} and V_{oc}, as well as FF lead to a low PCE of 2.7%. When LiF is added the contact is dramatically improved and the end result is a doubled PCE of 5.3%. When comparing the polymeric interlayers to LiF, PFN, PFN(EtOH)$_2$ and PBzFN had close to identical performance. This indicates that the tertiary amine functional group in these three polymers tuned the Al-electrode to a similar degree. In the case of PBzFN, it also shows the backbone does not affect the performance significantly. For the polymer PFIm, which had imidazole-functionalized side chains, a significant reduction in performance was seen. The V_{oc} and FF were unchanged while the current extraction was reduced. The EQE-curves show a similar trend. The bare Al-electrode devices are far below the others. PFIm improves it slightly and the rest of the interlayers were close to identical, with maximum efficiencies of around 55% in the two peaks at 470 nm and 630 nm.

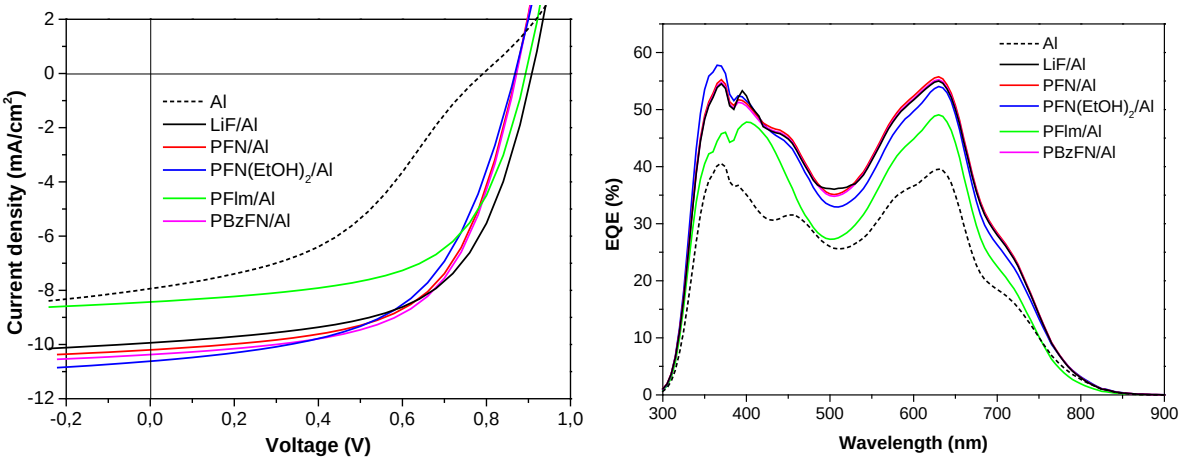

Figure 5.3. *J*–*V* curve and EQE curves for the all-PSCs.

Table 5.2. Device parameters of the all-PSCs.

Cathode	V_{oc} [V]	J_{sc} [mA/cm^2]	FF	PCE [%]
Al	0.79	7.9	0.43	2.7
LiF/Al	0.90	9.9	0.60	5.3
PFN/Al	0.87	10.2	0.60	5.3
PFN(EtOH)$_2$/Al	0.86	10.6	0.58	5.3
PFlm/Al	0.89	8.4	0.60	4.5
PBzFN/Al	0.87	10.4	0.60	5.4

The surface morphology of the films was studied using AFM. The resulting images, shown in figure 5.4, have almost identical surfaces with very similar roughness. This is not surprising, considering the extremely thin layers of the polymers.

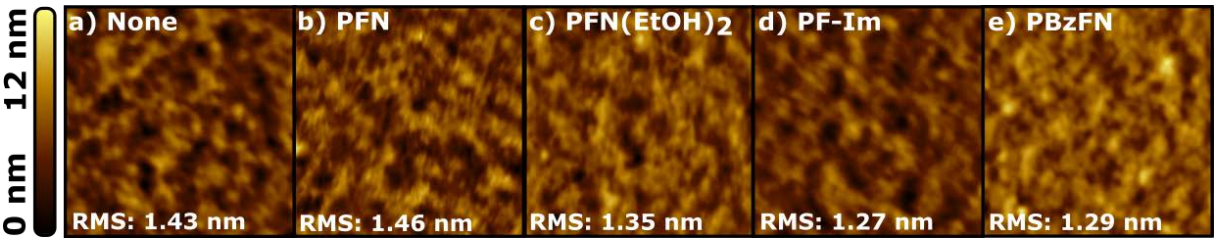

Figure 5.4. AFM images (2.5×2.5 µm) of (a) the naked active layer and (b-e) four interlayers on top of the active layer.

To further study the properties of the polymers, and to verify the presence of interlayers, surface contact angle measurements was performed. Five drops per film was used and the average of all angles is shown in figure 5.5. The resulting angles are significantly different from the naked active layer film, but the difference between the four interlayers are minimal, varying from 88.6 °to 92.0 °.

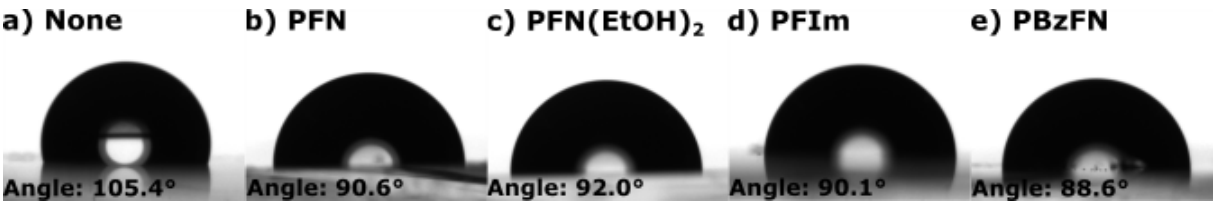

Figure 5.5. Contact angle measurements for (a) the naked active layer and (b-e) the four different interlayers.

This proves that the CIMs are present and that all four of the polymers reduce the hydrophobicity of the active layer surface, which should improve wettability between the active layer and the electrode.

6. Tertiary amine pendant group polymers

One way to introduce switchable solubility is to include amines into the solubilizing side chains. These can easily be oxidized, increasing the solubility in polar solvents dramatically.[55-57] By utilizing volatile acids, our hope is to process them and then evaporate the solvent together with the acid, regaining the original uncharged amine. Due to the negative effect on solar cell performance when highly polar groups such as hydroxyl or amine are included in the active layer, the studies of these materials as active layer components in solar cells are few and far in between.[56, 58-59]

Our hypothesis was that the oxidation potential of the donor polymer, related to the oxidation potential of the tertiary amine determined if efficient charge transfer could take place inside the polymer. This idea is supported by a few publications from the last few years.[56-57, 60] This study aimed to verify this, as well as to see if we could tailor the material to work in a satisfactory manner with the amines present. This is not such a strange idea, conventional electron transport supports that an amine that oxidizes far more easily than a polymer would form a charge trap, effectively stopping hole transport of the device.[61]

In order to study this, a series of seven polymers were synthesized and characterized. The polymers have not yet been tried in solar cell devices, but have undergone a series of characterization methods to study their electrochemical and optical properties. In some cases, the film forming ability has been studied using TEM and AFM.

To make the polymers comparable to conventional polymers without tertiary amine pendant groups, three commonly used moieties were chosen. These were BTz, DPP and II. The monomer synthesis pathways are shown in figure 6.1.

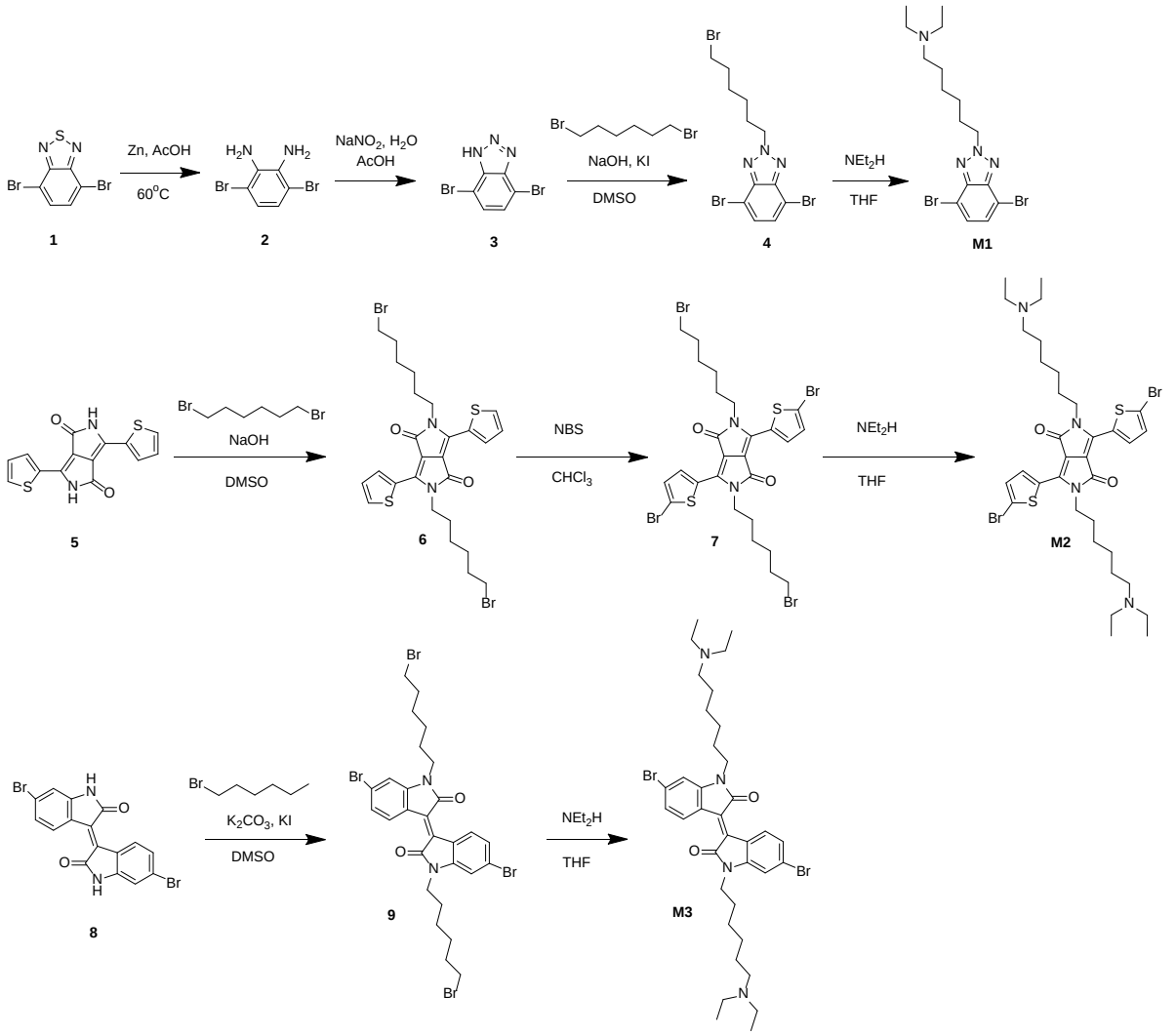

Figure 6.1. Synthesis of tertiary amine pendant group monomers **M1**, **M2** and **M3.**

In the case of benzotriazole the synthesis pathway was longer, since it included the reductive ring opening of benzothiadiazole and ring closing with sodium nitrite. The next step was similar for all three monomers and was an alkylation reaction with 1,6-dibromohexane. These reactions turned out to require drastically different conditions. After a large amount of trial and error, the BTz and DPP moieties turned out to require sodium hydroxide while isoindigo degraded under the same conditions. After the alkylation step the DPP monomer required bromination. The last step for all three was to introduce the tertiary amine group. Due to the relatively short hexyl chain, it was judged diethyl amine was suitable to increase solubility. These reactions were simple to perform, but the final monomer purification was challenging in all three cases. Several steps of chromatography over neutral aluminium oxide and subsequent recrystallization with various solvents were required. The following polymers were performed by both Stille and Suzuki reactions, as can be seen in figure 6.2.

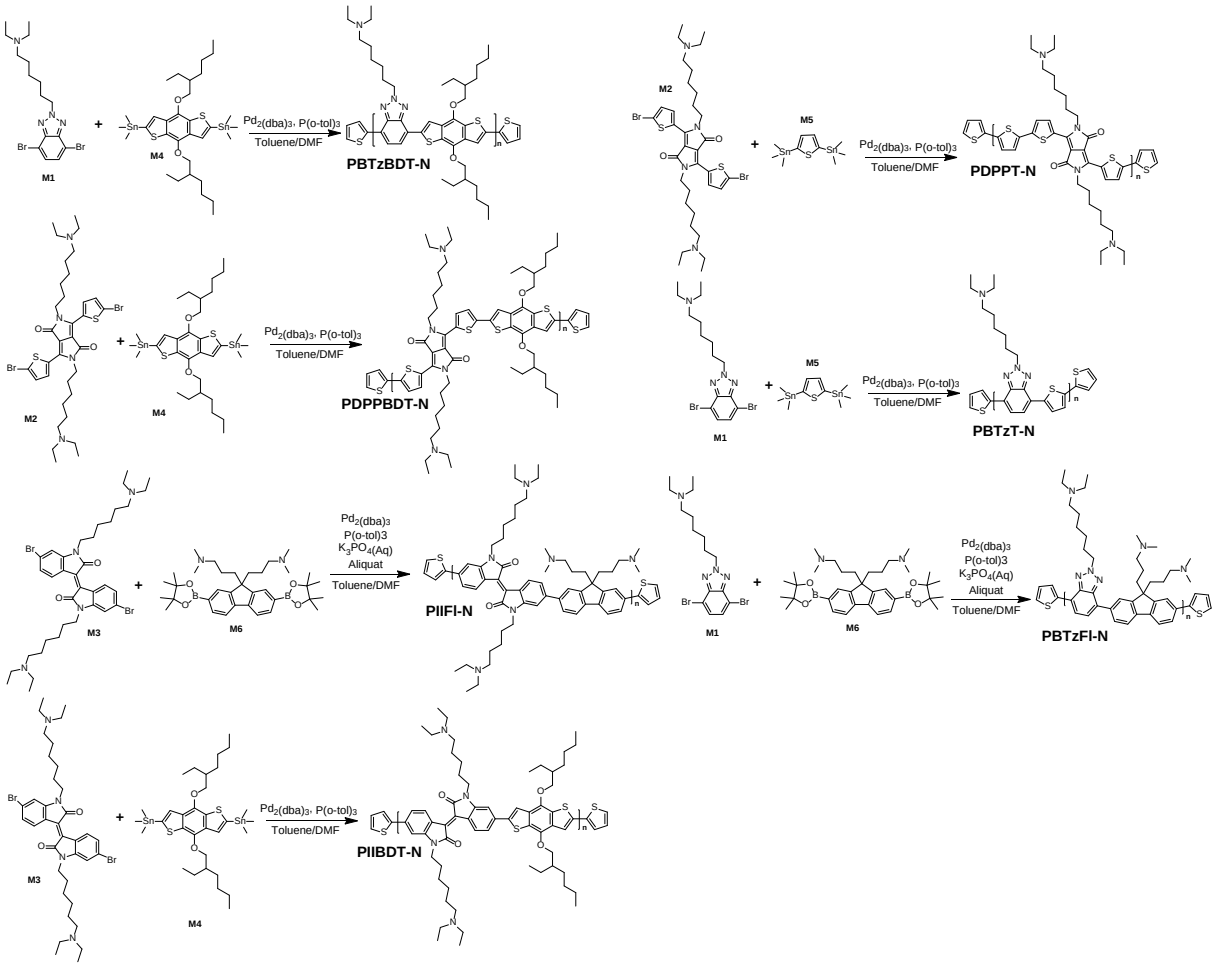

Figure 6.2. Polymerization reactions for the seven copolymers, PBTzBDT-N, PDPPT-N, PDPPBDT-N, PBTzT-N, PIIFl-N, PBTzFl-N and PIIBDT-N.

In all these cases the second monomer was a commercially available monomer that were used as received from vendor. Generally, the polymerization reactions were performed under inert atmosphere, around 100 °C in anhydrous toluene/DMF 10:1 solvent mixture. The monomers, catalyst and co-catalyst solids were mixed in a round bottom flask, held under vacuum for 30 min and then dissolved in degassed solvent and further degassed for a few minutes. The Suzuki reactions were also injected with 2 M K_3PO_4(Aq) and a few drops of Aliquat 336. They were then heated and stirred vigorously until judged complete, which varies from five minutes to three days. The polymers were then precipitated from hexane, filtered into a soxhlet thimble, successively cleaned with petroleum ether, diethyl ether, and acetone and then extracted with chloroform. The chloroform solution was passed through short neutral alumina columns and then precipitated from hexane again. The solids were filtered, dried and collected.

Electrochemical characterization using CV as well as SWV took place for all seven polymers and is shown in figure 6.3 and the HOMO and LUMO levels are illustrated in an energy level diagram in figure 6.4.

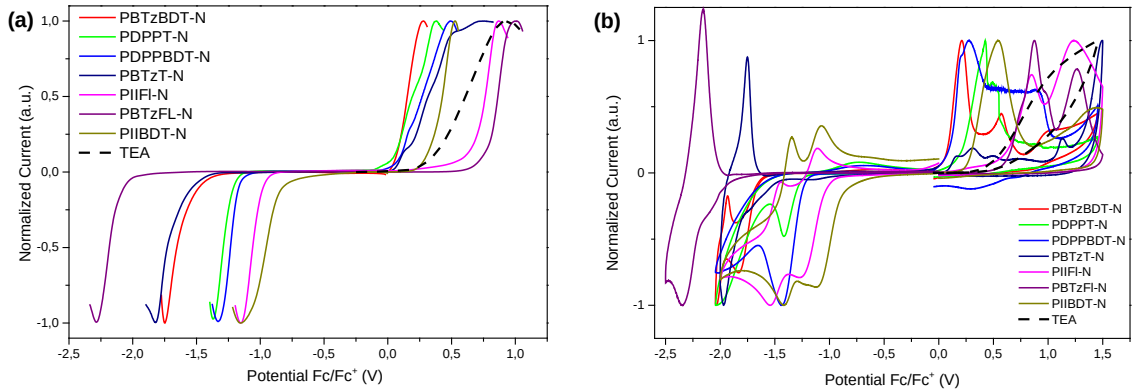

Figure 6.3. a) SWV and b) CV for the seven polymers.

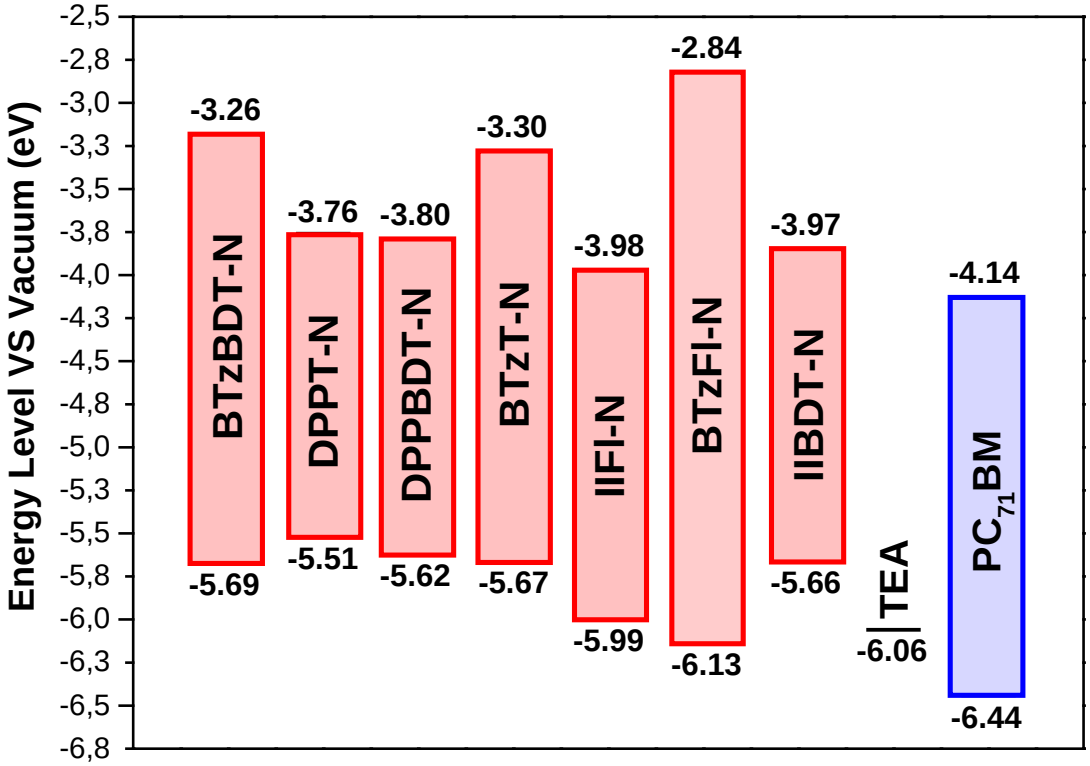

Figure 6.4. Energy level of the seven donor polymers measured by square wave voltammetry.

Optical properties measured by UV-Vis gave spectra of staggered absorption for the different polymers. Since the aim was to make polymers with a wide variety of band gaps, this was expected. The absorption can be seen in figure 6.5.

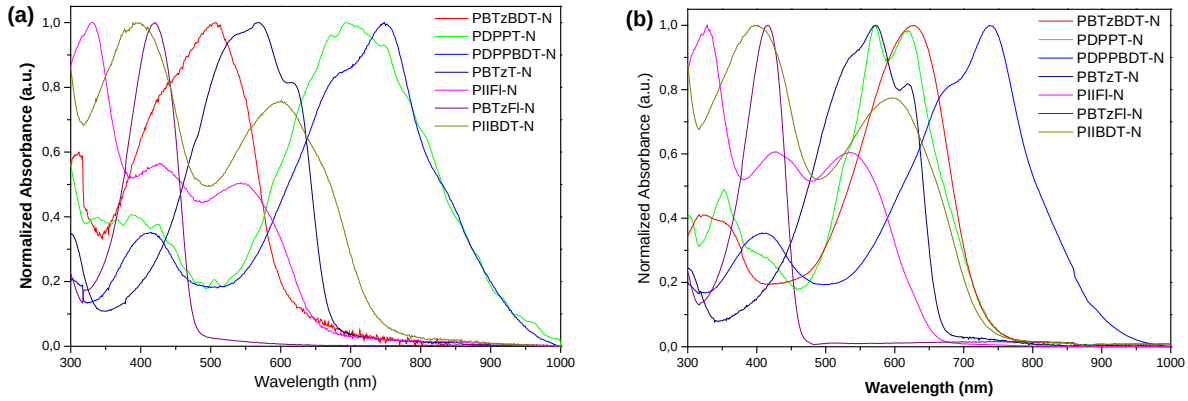

Figure 6.5. (a) Normalized UV-Vis absorption spectra of polymers in film. (b) Normalized UV-Vis absorption spectra of polymers in solution.

For some of the polymers, PBTzBDT-N, PDPPT-N, PDPPBDT-N and PIIFl-N, there is a small secondary oxidation peak at around 0.5 V potential. This is likely the oxidation of the pendant tertiary amine. This could possibly be dependent on the strength of transition, meaning the strongly allowed electron transitions of the polymers which do not show the amine oxidation drench out the weak amine oxidation. Table 6.1 presents a summary of the optical properties and the electrochemical properties determined by SWV.

Table 6.1. Optical and electrochemical properties of the copolymers.

	UV–Vis absorption				SWV		
	Solution	Film					
Polymer	λ_{max}[a] (nm)	λ_{max}[b] (nm)	λ_{onset} (nm)	E_g^{opt} (eV)[c]	HOMO (eV)	LUMO (eV)	E_g^{ec} (eV)[d]
PBTzBDT-N	625	504	601	2.07	–5.40	–3.49	1.91
PDPPT-N	571	697	934	1.32	–5.51	–3.76	1.75
PDPPBDT-N	738	751	940	1.32	–5.62	–3.80	1.82
PBTzT-N	569	569	671	1.85	–5.67	–3.30	2.37
PIIFl-N	328	330	644	1.92	–5.99	–3.98	2.01
PBTzFl-N	415	425	482	2.58	–6.13	–2.84	3.29
PIIBDT-N	396	400	727	1.71	–5.66	–3.97	1.69

[a]Absorption maximum in chloroform solution; [b]Absorption maximum in film; [c]Optical band gap; [d]Electrochemical band gap.

In previous publications, the oxidation peak of the tertiary amine has been observed for some polymers, while in others it is not observed.[56] To analyze this effect, we decided to compare

two different methods of electrochemistry. The common methods SWV and CV were employed and analyzed together. A trend can be observed in the resulting voltammogrammes, seen in figure 6.6, where SWV and CV for the polymers are compared to measurements of triethylamine.

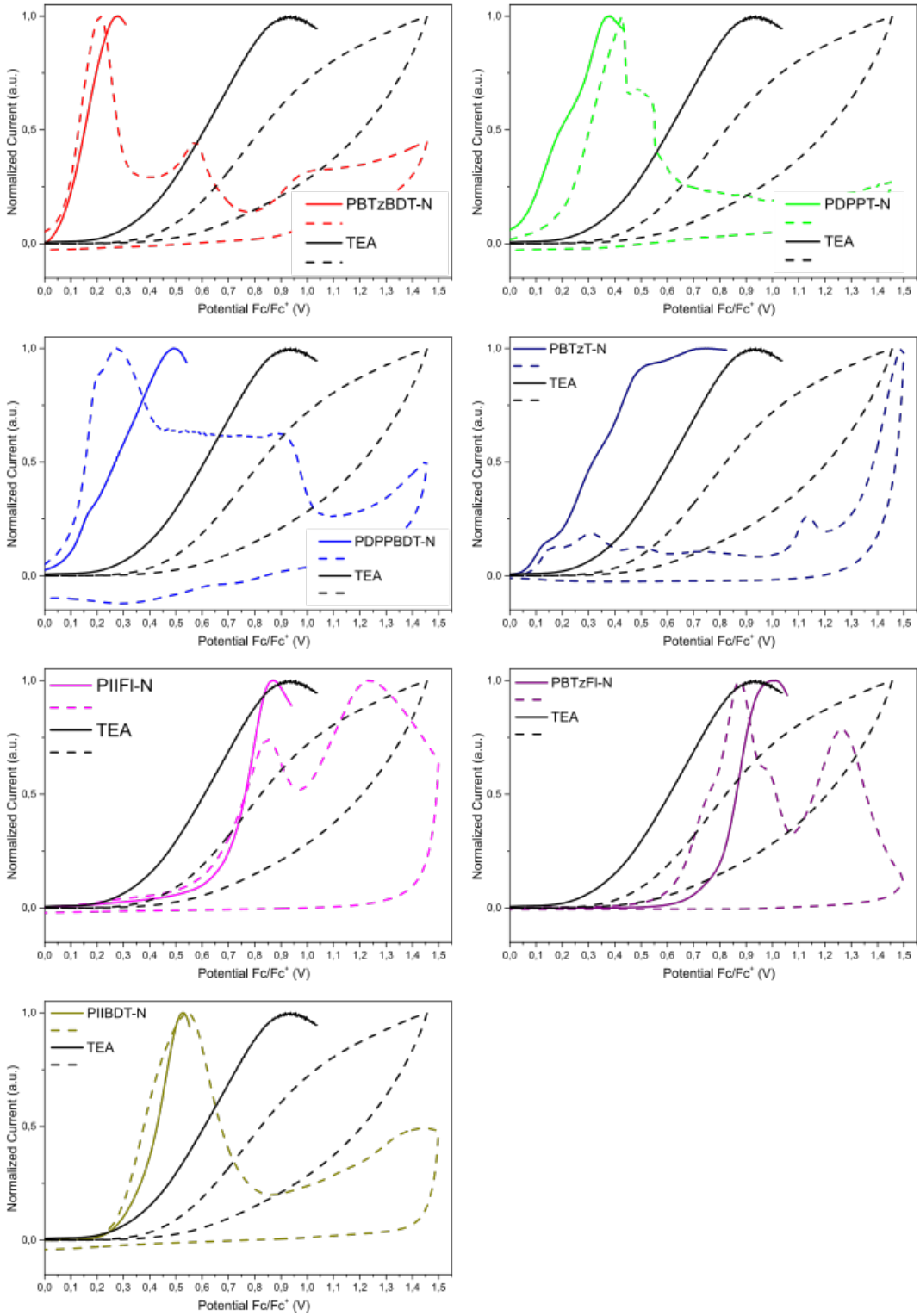

Figure 8. Comparison of oxidation measured by SWV (solid lines) and CV (dashed lines) for all seven polymers with TEA as a reference.

Due to the difference in method between SWV and CV, it is important to differentiate between the data. For SWV the oxidation potential is calculated for the peaks, while for CV the onset of oxidation is used. Several of the polymers exhibit oxidation potentials lower than that of the TEA, and in these cases the SWV peak is not helpful since the measurement is stopped at the first peak. This seems to be the case for all polymers except PIIFl-N and PBTzFL-N and possibly a double peak found for PBTzT-N. These former two polymers were designed to have a deep HOMO level, which is represented in their oxidation potential. For these two polymers, the SWV peaks correspond well with that of TEA. Thus it is quite likely the reported energy levels were incorrect, and the second oxidation peaks seen in the CV should be used instead. Secondary oxidation peaks in the CV show up in some of the other polymers, but it is harder to judge when using the onset in an already oxidized state. The polymers with likely side chain oxidation are PBTzBDT-N, PDPPT-N, PDPPBDT-N and most likely PBTzT-N. The last polymer, PIIBDT-N, seems to show no tendency of a secondary oxidation peak close to that of TEA. PBTzBDT-N and PDPPBDT-N were chosen for further study in blends with $PC_{71}BM$, using TEM and AFM. The results are shown in figure 6.7.

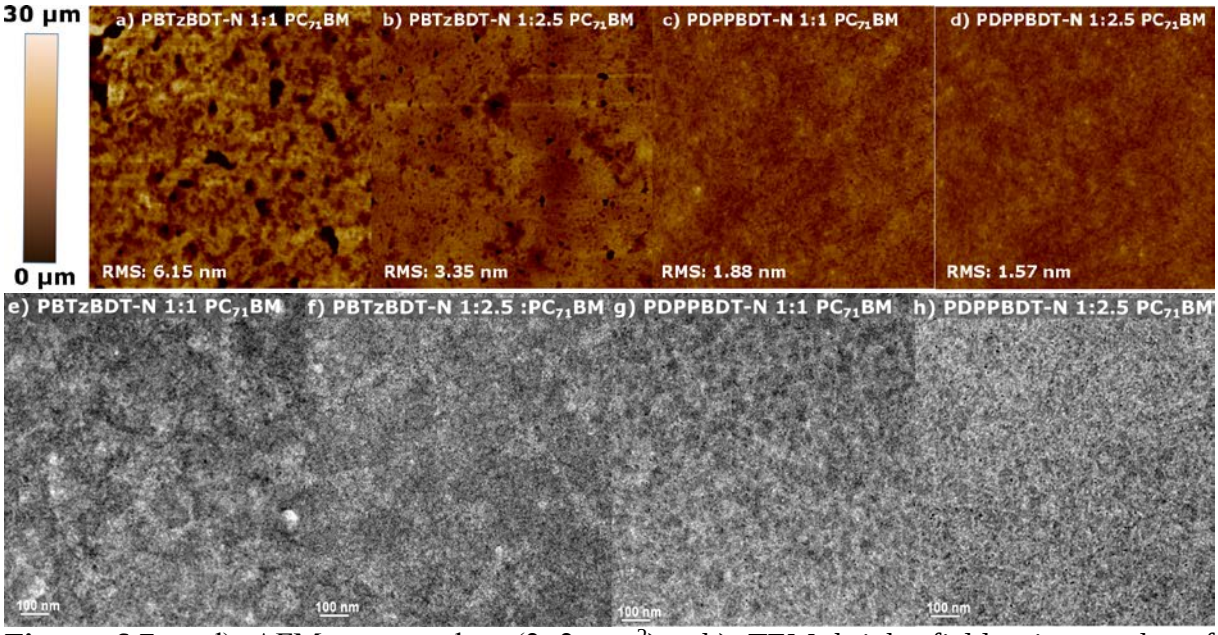

Figure 6.7. a-d) AFM topography, (2×2 μm^2) e-h) TEM bright field micrographs of polymer:$PC_{71}BM$ blends.

As seen in the AFM images, and the TEM micrographs, PBTzBDT-N seems to form a rougher morphology with domains at the 100 nm scale, while PDPPBDT-N forms smaller domains.

After the seven polymers were exposed to several series of screening in solar cell devices with various treatments, a couple of polymers showed higher than the expected ~0% in device performance. These were PBDTzBDT-N and PDPPBDT-N. To study this in a systematic way

a series of solar cells were produced from them, as well as a second batch of PBTzBDT-N called PBTzBDT-Nb. This polymer seemed to exhibit slightly higher molecular weight as well as solubility. Table 6.2 shows a summary of the device performance, as an average of six devices, with a few different device configurations. The conventional device structure used was: ITO/MoOx/Polymer:$PC_{71}BM$/LiF/Ag and the inverted device structure was: ITO/ZnO/Polymer:$PC_{71}BM$/MoOx/Ag where some devices also included an interlayer between the ITO/ZnO cathode and the active layer.

Table 6.2. Photovoltaic parameters of devices fabricated using Polymer:$PC_{71}BM$ (1:2.5) bulk heterojunction. The average is from six identical devices.

Polymer	J_{SC} **(mA cm^{-2})**	**FF (%)**	V_{OC} **(V)**	**PCE (%)**
PBTzBDT-N:$PC_{71}BM$[a]	3.1 (2.98 ± 0.13)	42 (41 ± 1)	0.83 (0.82 ± 0.01)	1.01 (1 ± 0.02)
PBTzBDT-N:$PC_{71}BM$[b]	2.72 (2.57 ± 0.1)	40 (40 ± 0.5)	0.88 (0.86 ± 0.02)	0.94 (0.87 ± 0.04)
PBTzBDT-N:$PC_{71}BM$[c]	2.15 (1.85 ± 0.5)	38 (36 ± 1)	0.82 (0.79 ± 0.03)	0.61 (0.53 ± 0.04)
PBTzBDT-Nb:$PC_{71}BM$	2.4 (2.25 ± 0.1)	43 (41 ± 2)	0.37 (0.34 ± 0.02)	0.34 (0.31± 0.02)
PBTzBDT-Nb:$PC_{71}BM$	2.25 (2.57 ± 0.1)	37 (36 ± 0.5)	0.51 (0.50 ± 0.01)	0.41 (0.38 ± 0.03)
PBTzBDT-Nb:$PC_{71}BM$[d]	1.24 (1± 0.14)	27 (26± 0.4)	0.45 (0.44± 0.02)	0.14 (0.11± 0.01)
PDPPBDT-N:$PC_{71}BM$[a]	1.08 (1 ± 0.05)	34 (32 ± 1)	0.13 (0.12 ± 0.01)	0.04 (0.04± 0.00)
PDPPBDT-N:$PC_{71}BM$[b]	1.64 (1.52 ± 0.06)	35 (34 ± 0.5)	0.34 (0.33 ± 0.01)	0.18 (0.17 ± 0.07)
PDPPBDT-N:$PC_{71}BM$[c]	1.65 (1.38± 0.13)	38 (36± 3)	0.34 (0.32± 0.03)	0.21 (0.16± 0.03)

[a)]Inverted device without TPD [b)]Inverted device with TPD [c)]Conventional device with MoO_x
[d)]Conventional device with PEDOT:PSS

7. Conclusion and Outlook

In this thesis, a variety of conjugated polymers were presented with the common theme of side-chain modification. These show what a flexible method side-chain engineering can be to affect the properties of conjugated polymers. Three studies were presented with the focus on morphological analysis using TEM. The three different studies presented illustrated what a powerful tool TEM can be to characterize thin films of organic material. In the first case, a polymer had the alkyl side chains moved one position on a phenyl-ring, resulting in dramatic morphological differences. Two of the polymers were also fluorinated on the electron-deficient quinoxaline unit, which gave severe phase separation for both polymers. These effects were clearly visible in the presented micrographs. The second case illustrated a case where TEM was less useful. Due to very fine intermixing the micrographs were mostly gray noise and not much information could be gained. In the third case, TEM was used to find the optimal morphology range for a polymer:PCBM system. These are interesting examples where TEM has been used to gain information in PSCs. Unfortunately, it seems like the future of PSCs might be in either all-PSCs or devices with small molecule acceptors. Neither of these generate much contrast to the donor polymer, which means TEM might lose its importance.

In chapter 4, a series of polymers bearing thermocleavable sidechains was presented. Based on the results of the TEM- and AFM analysis, BOC protection was shown to be a practical and simple way to produce insoluble polymer films from processable polymers. The morphology study here showed that the induced hydrogen bonding stops phase separation and PCBM-crystallization. Utilization of this effect to get long term stability seems like an attractive design. Due to the good solubility before heating and the insolubility after, there are many other possible applications for these materials outside of PSCs.

In the following section, four different polymers were synthesized, characterized and used as cathode interlayers in all-PSCs. The polymers had three different pendant groups and two backbone configuration, to study the effect of these on device performance. All polymers significantly improved the performance when compared to bare Al-electrode and the three polymers with tertiary amine pendant groups showed almost identical performance to the conventional LiF-layer. These results show that the backbone structure is less important, since PFN and PBzFN has identical performance. The last polymer, containing an imidazole pendant group, was slightly less effective. On the other hand, this polymer showed a higher degree of thermal stability. Interfacial layer polymers for all-PSCs is a detail which needs to be further

studied. The polymers presented in this study performed well, but not above that of the benchmark polymer PFN.

In the last section, seven polymers bearing tertiary amine sidechains were presented. The aim was to produce alcohol-/water processable polymers with staggered energy levels to see if it would affect the generally poor device performance when tertiary amines are present in the active layers. Using different monomer combinations, the difference in energy levels gave staggered absorption spectra and oxidation-/reduction potentials. To carefully analyze the electrochemical properties, both CV and SWV were used and in some of the polymers, it was possible to see a small secondary oxidation in the same position, around 0.5 V. This is attributed to the tertiary amine oxidation. The polymers were screened in solar cells to see if any performance was seen, and in depth study for three polymers was performed. One polymer showed a steady efficiency of ~1% but the fundamental reasons to why one polymer works the others do not is still not clear. Even though it is likely the solar cell performance will always be lackluster at best, they still might be useful in other application where the amine might be useful, instead of harmful.

Bibliography

[1] IEA, in *World Energy Outlook Special Report*, **2015**
[2] S. Lizin, S. Van Passel, E. De Schepper, W. Maes, L. Lutsen, J. Manca and D. Vanderzande, *Energy Environ. Sci.* **2013**, *6*, 3136.
[3] S. B. Darling and F. You, *RSC Adv.* **2013**, *3*, 17633.
[4] N. Thejo Kalyani and S. J. Dhoble, *Renew. Sust. Energy. Rev.* **2012**, *16*, 2696-2723.
[5] G. H. Kim, L. Shao, K. Zhang and K. P. Pipe, *Nat. Mater.* **2013**, *12*, 719-723.
[6] J. Mei, Y. Diao, A. L. Appleton, L. Fang and Z. Bao, *J. Am. Chem. Soc.* **2013**, *135*, 6724-6746.
[7] G. Li, R. Zhu and Y. Yang, *Nat. Photonics.* **2012**, *6*, 153-161.
[8] S. Günes, H. Neugebauer and N. S. Sariciftci, *Chem. Rev.* **2007**, *107*, 1324-1338.
[9] S. Subianto, N. Dutta, M. Andersson and N. R. Choudhury, *Adv. Colloid. Interface. Sci.* **2016**, *235*, 56-69.
[10] B. C. Thompson and J. M. Frechet, *Angew. Chem. Int. Ed. Engl.* **2008**, *47*, 58-77.
[11] E. Bundgaard and F. Krebs, *Sol. Energy Mater. Sol. Cells* **2007**, *91*, 954-985.
[12] T. Huld, R. Müller and A. Gambardella, *Sol. Energy* **2012**, *86*, 1803-1815.
[13] M. Šúri, T. A. Huld, E. D. Dunlop and H. A. Ossenbrink, *Sol. Energy* **2007**, *81*, 1295-1305.
[14] E. J. L. Hideki Shirakawa, Alan G. MacDiarmid, Chwan K. Chiang, Alan J. Heeger, *J.C.S. Chem. Comm.* **1977**, 578-580.
[15] H. A. M. Van Mullekom, J. A. J. M. Vekemans, E. E. Havinga and E. W. Meijer, *Mater. Sci. Eng.* **2001**, *32*, 1-40.
[16] J. G. G. Yu, J. C. Hummelen, F. Wudl, A. J. Heeger, *Science* **1995**, *270*, 1789-1791.
[17] W. Zhao, S. Li, H. Yao, S. Zhang, Y. Zhang, B. Yang and J. Hou, *J. Am. Chem. Soc.* **2017**, *139*, 7148-7151.
[18] W. Zhao, D. Qian, S. Zhang, S. Li, O. Inganas, F. Gao and J. Hou, *Adv. Mater.* **2016**, *28*, 4734-4739.
[19] Z. Zheng, O. M. Awartani, B. Gautam, D. Liu, Y. Qin, W. Li, A. Bataller, K. Gundogdu, H. Ade and J. Hou, *Adv. Mater.* **2017**, *29*.
[20] G. Zhang, K. Zhang, Q. Yin, X. F. Jiang, Z. Wang, J. Xin, W. Ma, H. Yan, F. Huang and Y. Cao, *J. Am. Chem. Soc.* **2017**, *139*, 2387-2395.
[21] F. C. Krebs, *Sol. Energy Mater. Sol. Cells* **2009**, *93*, 394-412.
[22] B. Kippelen and J.-L. Brédas, *Energy Environ. Sci.* **2009**, *2*, 251.
[23] B. Qi and J. Wang, *Phys. Chem. Chem. Phys.* **2013**, *15*, 8972-8982.
[24] J. M. G. Cowie and V. Arrighi, *Polymers: Chemistry and Physics of Modern Materials*, CRC Press, **2007**.
[25] J. M. Hollas, *Modern Spectroscopy, 4th Edition*, Wiley, **2003**.
[26] C. M. Cardona, W. Li, A. E. Kaifer, D. Stockdale and G. C. Bazan, *Adv. Mater.* **2011**, *23*, 2367-2371.
[27] A. J. Bard and L. R. Faulkner, *Electrochemical Methods: Fundamentals and Applications*, Wiley, **2000**.
[28] F. Z. S. Hellström, O. Inganäs, M. R. Andersson, *Dalton Trans.* **2009**, 10032-10039.
[29] R. J. Good, *J. Adhesion Sci. Technol.* **1992**, *6*, 1269-1302.
[30] J. K. van Duren, Yang, X., Loos, J., Bulle-Lieuwma, C.W., Sieval, A.B., Hummelen, J.C. and Janssen, R.A.,, *Adv. Funct. Mater.* **2004**, *14*, 425-434.
[31] S. S. van Bavel, M. Bärenklau, G. de With, H. Hoppe and J. Loos, *Adv. Funct. Mater.* **2010**, *20*, 1458-1463.
[32] M. Pfannmoller, H. Flugge, G. Benner, I. Wacker, C. Sommer, M. Hanselmann, S. Schmale, H. Schmidt, F. A. Hamprecht, T. Rabe, W. Kowalsky and R. R. Schroder, *Nano Letters* **2011**, *11*, 3099-3107.
[33] J. Jo, S.-S. Kim, S.-I. Na, B.-K. Yu and D.-Y. Kim, *Adv. Funct. Mater.* **2009**, *19*, 866-874.
[34] C. Lindqvist, J. Bergqvist, O. Bäcke, S. Gustafsson, E. Wang, E. Olsson, O. Inganäs, M. R. Andersson and C. Müller, *Appl. Phys. Lett.* **2014**, *104*, 153301.

[35] L. Derue, O. Dautel, A. Tournebize, M. Drees, H. Pan, S. Berthumeyrie, B. Pavageau, E. Cloutet, S. Chambon, L. Hirsch, A. Rivaton, P. Hudhomme, A. Facchetti and G. Wantz, *Adv. Mater.* **2014**, *26*, 5831-5838.
[36] O. Backe, C. Lindqvist, A. Diaz de Zerio Mendaza, S. Gustafsson, E. Wang, M. R. Andersson, C. Muller and E. Olsson, *Nanoscale* **2015**, *7*, 8451-8456.
[37] J. L. Brusso, M. R. Lilliedal and S. Holdcroft, *Polym. Chem.* **2011**, *2*, 175-180.
[38] H. S. Frederik C. Krebs, *Chem. Mater.* **2005**, *17*, 5235-5237.
[39] Z.-H. Guo, N. Ai, C. R. McBroom, T. Yuan, Y.-H. Lin, M. Roders, C. Zhu, A. L. Ayzner, J. Pei and L. Fang, *Polym. Chem.* **2016**, *7*, 648-655.
[40] M. Helgesen, S. A. Gevorgyan, F. C. Krebs and R. A. J. Janssen, *Chem. Mater.* **2009**, *21*, 4669-4675.
[41] M. Helgesen, R. Søndergaard and F. C. Krebs, *J. Mater. Chem.* **2010**, *20*, 36-60.
[42] E. N. K. Jinsong Liu, Yuxiang Liu, Michael D. McGehee, Jean M. J. Fréchet, *J. Am. Chem. Soc.* **2004**, *126*, 9486-9487.
[43] C. Liu, S. Dong, P. Cai, P. Liu, S. Liu, J. Chen, F. Liu, L. Ying, T. P. Russell, F. Huang and Y. Cao, *ACS Appl. Mater. Interfaces* **2015**, *7*, 9038-9051.
[44] C. Liu, W. Xu, Q. Xue, P. Cai, L. Ying, F. Huang and Y. Cao, *Dyes Pigments* **2016**, *125*, 54-63.
[45] R. Søndergaard, M. Helgesen, M. Jørgensen and F. C. Krebs, *Adv. Energy Mater.* **2011**, *1*, 68-71.
[46] F. C. K. H. Spanggaard, *Chem. Mater.* **2005**, *17*, 5235-5237.
[47] B. Sun, W. Hong, H. Aziz and Y. Li, *J. Mater. Chem.* **2012**, *22*, 18950.
[48] P. Vahdani, X. Li, C. Zhang, S. Holdcroft and B. J. Frisken, *J. Mater. Chem. A* **2016**, *4*, 10650-10658.
[49] M. Jorgensen, K. Norrman, S. A. Gevorgyan, T. Tromholt, B. Andreasen and F. C. Krebs, *Adv. Mater.* **2012**, *24*, 580-612.
[50] B. W. Arnold B. Tamayo, and Thuc-Quyen Nguyen, *J. Phys. Chem. C* **2008**, *112*, 11545–11551.
[51] Z. He, C. Zhong, S. Su, M. Xu, H. Wu and Y. Cao, *Nat. Photonics.* **2012**, *6*, 593-597.
[52] Z. He, C. Zhong, X. Huang, W. Y. Wong, H. Wu, L. Chen, S. Su and Y. Cao, *Adv. Mater.* **2011**, *23*, 4636-4643.
[53] T.-H. Lai, S.-W. Tsang, J. R. Manders, S. Chen and F. So, *Mater. Today* **2013**, *16*, 424-432.
[54] P. F. El Hadj Elandaloussi, Pascal Richomme, J. Orduna, J. Garin, Jean Roncali, *J. Am. Chem. Soc.* **1997**, *119*, 10774-10784.
[55] Z. Hu, K. Zhang, F. Huang and Y. Cao, *Chem. Commun.* **2015**, *51*, 5572-5585.
[56] C. Duan, W. Cai, B. B. Y. Hsu, C. Zhong, K. Zhang, C. Liu, Z. Hu, F. Huang, G. C. Bazan, A. J. Heeger and Y. Cao, *Energy Environ. Sci.* **2013**, *6*, 3022.
[57] Z. George, Y. Xia, A. Sharma, C. Lindqvist, G. Andersson, O. Inganäs, E. Moons, C. Müller and M. R. Andersson, *J. Mater. Chem. A* **2016**, *4*, 2663-2669.
[58] Z. Zhong, Z. Hu, Z. Jiang, J. Wang, Y. Chen, C. Song, S. Han, F. Huang, J. Peng, J. Wang and Y. Cao, *Adv. Electron. Mater.* **2015**, *1*, 1400014.
[59] M. Lv, M. Lei, J. Zhu, T. Hirai and X. Chen, *ACS Appl. Mater. Interfaces* **2014**, *6*, 5844-5851.
[60] W. Cai, C. Zhong, C. Duan, Z. Hu, S. Dong, D. Cao, M. Lei, F. Huang and Y. Cao, *Appl. Phys. Lett.* **2015**, *106*, 233302.
[61] T. M. Clarke and J. R. Durrant, *Chem. Rev.* **2010**, *110*, 6736–6767.